0026-895X/02/6104-817–831$7.00
MOLECULAR PHARMACOLOGY
Vol. 61, No. 4
1294/969726
Mol Pharmacol 61:817–831, 2002
Printed in U.S.A.
Copyright © 2002 The American Society for Pharmacology and Experimental Therapeutics

Regulation of Extracellular Signal-Regulated Kinase Cascades by α- and β-Isoforms of the Human Thromboxane A_2 Receptor

SINEAD M. MIGGIN and B. THERESE KINSELLA

Department of Biochemistry, Conway Institute of Biomolecular and Biomedical Research, University College Dublin, Dublin, Ireland

Received August 13, 2001; accepted December 22, 2001
This article is available online at http://molpharm.aspetjournals.org

ABSTRACT

Thromboxane A_2 (TXA_2) stimulates mitogenic growth of vascular smooth muscle. In humans, TXA_2 signals through two TXA_2 receptor (TP) isoforms, termed TPα and TPβ. To investigate the mechanism of TXA_2-mediated mitogenesis, regulation of extracellular signal-regulated kinase (ERK) signaling was examined in human embryonic kidney 293 cells stably overexpressing the individual TP isoforms. The TXA_2 mimetic 9,11-dideoxy-9α,11α-methano epoxy prostaglandin $F_{2\alpha}$ (U46619) elicited concentration- and time-dependent activation of ERK1 and -2 through both TPs with maximal TPα- and TPβ-mediated ERK activation observed after 10 and 5 min, respectively. U46619-mediated ERK activation was inhibited by the TP antagonist [1*S*-[1α,2β-(5*Z*)-3β,4α-]]-7-[3-[[2-(phenylamino)carbonyl]hydrazine] methyl]-7-oxabicyclo[-2,2,1-]hept-2yl]-5-heptenoic acid (SQ29,548), and by the mitogen-activated protein kinase kinase inhibitor 2′-amino-3′-methoxyflavone (PD 98059). Although ERK activation through TPα was dependent on 2-[1-(dimethylaminopropyl)-1H-indol-3-yl]-3-(1H-indol-3-yl)-maleimide (GF 109203X)-sensitive protein kinase (PK) Cs, ERK activation through TPβ was only partially dependent on PKCs. ERK activation through both TPα and TPβ was dependent on PKA and phosphoinositide 3-kinase (PI3K) class 1_A, but not class 1_B, and was modulated by Harvey-Ras, A-Raf, c-Raf, and Rap1B/B-Raf and also involved transactivation of the epidermal growth factor receptor. Additionally, PKB/Akt was activated through TPα and TPβ in a PI3K-dependent manner. In conclusion, we have defined the key components of TXA_2-mediated ERK signaling and have established that both TPα and TPβ are involved. TXA_2-mediated ERK activation through the TPs is a complex event involving PKC-, PKA-, and PI3K-dependent mechanisms in addition to transactivation of the EGF receptor. TPα and TPβ mediate ERK activation through similar mechanisms, although the time frame for maximal ERK activation and PKC dependence differs.

The prostanoid thromboxane A_2 (TXA_2) mediates a number of cellular responses, including platelet aggregation and contraction of vascular smooth muscle (Narumiya et al., 1999). TXA_2 may stimulate mitogenic and/or hypertrophic growth of vascular smooth muscle (Morinelli et al., 1994), and a number of studies have shown that the TXA_2 mimetic U46619 elicits extracellular signal-regulated kinase (ERK) activation in porcine, rat, bovine, and human smooth muscle cells, respectively (Morinelli et al., 1994; Jones et al., 1995; Grosser et al., 1997; Miggin and Kinsella, 2001).

The TXA_2 receptor (TP), a member of the G protein-coupled receptor (GPCR) superfamily, is primarily coupled to Gq-dependent activation of phospholipase (PL) C (Narumiya et al., 1999). Previous studies have shown that down-regulation of diacyl glycerol (DAG)-regulated protein kinase (PK) C isozymes inhibits the ability of the G_q-coupled GPCRs to activate ERK signaling (Bogoyevitch et al., 1994). This effect is mediated through the ubiquitously expressed serine/threonine kinase c-Raf (Hagemann and Rapp, 1999). c-Raf, the most studied member of the Raf family, which also includes A-Raf and B-Raf, interacts directly with GTP-bound Ras, activating the ERK signaling cascade (Hagemann and Rapp, 1999). The Raf isoforms may be differentially regulated in response to diverse stimuli (Hagemann and Rapp, 1999); for example, although c-Raf is inhibited by cAMP-dependent

This study was supported by Enterprise Ireland, The Wellcome Trust, The Health Research Board of Ireland, and The Irish Heart Foundation.

ABBREVIATIONS: TXA_2, thromboxane A_2; ERK, extracellular signal-regulated kinase; TP, thromboxane A_2 receptor; GPCR, G protein-coupled receptor; PL, phospholipase; DAG, diacyl glycerol; PK, protein kinase; PI3K, phosphoinositide 3-kinase; SH, src-homology; PG, prostaglandin; PD 98059, 2′-amino-3′-methoxyflavone; GF 109203X, 2-[1-(3-dimethylaminopropyl)-1H-indol-3-yl]-3-(1H-indol-3-yl)-maleimide; Tyrphostin AG 1478, 4-(3-chloroanilino)-6,7-dimethoxyguinazoline; PP2, 4-amino-5-(4-chlorophenyl)-7-(*t*-butyl)pyrazolo[3,4-*d*]pyramidine; H-89, {*N*-[2-((*p*-bromocinnamyl)amino)ethyl]-5-isoquinolinesulfonamide, 2HCl; U46619, 9,11-dideoxy-9α,11α-methano epoxy prostaglandin $F_{2\alpha}$; KT5720, (8*R*,9*S*,11*S*)-(−)-9-hydroxy-9-hexoxycarbonyl-8-methyl-2,3,9,10-tetrahydro-8,11-epoxy-1H,8H,11H-2,7b,11a-triazadibenzo[*a*,*g*]cycloocta[*cde*]trinden-1-one; HA, hemagglutinin; Ha-Ras, Harvey Ras; MBP, myelin basic protein; PMA, phorbol-12-myristate-13-acetate; DN, dominant negative; KD, kinase dead; HEK, human embryonic kidney; MEM, minimal essential medium; FBS, fetal bovine serum; PBS, phosphate-buffered saline; PVDF, polyvinylidene difluoride; ppERK, phosphorylated extracellular signal-regulated kinase; ppPKB, phosphorylated protein kinase B; PAGE, polyacrylamide gel electrophoresis; PTx, pertussis toxin; SMC, smooth muscle cell.

PKA, A-Raf is insensitive (Hagemann and Rapp, 1999; Sutor et al., 1999). On the other hand, PKA not only blocks c-Raf activation but also may phosphorylate the low-molecular-mass guanine nucleotide binding protein Rap 1, which in turn recruits and causes sustained activation of B-Raf (Schmitt and Stork, 2000).

Phosphoinositide 3-kinase (PI3K) has been identified as one of the main mediators of growth factor-regulated cell proliferation and cell survival, transmitting antiapoptotic signals. The PI3K class I_A family members consist of a p110α, β, or δ catalytic subunit and a p85α or β adaptor subunit. Growth factor stimulation of cells is mediated in part by interaction of the src-homology (SH)2 domains of the p85 adaptor subunits with tyrosine-phosphorylated proteins, such as receptor tyrosine kinases and growth factor receptor binding protein-2 (Wang et al., 1995; Sugden and Clerk, 1997). The PI3K class I_B family, consisting of a p110γ catalytic subunit, is stimulated by G protein $\beta\gamma$ subunits and does not interact with SH2 domain-containing adaptors (Lopez-Ilasaca et al., 1998). Both class I_A and I_B PI3Ks interact with GTP-bound Ras, which can act as both an effector and regulator of PI3K (Sugden and Clerk, 1997). Several studies suggest that PKB/Akt activation, by complex formation with the phosphatidyl inositol-3,4,5-trisphosphate lipid products of PI3K, is a key event in the realization of the antiapoptotic effect of PI3K (Datta et al., 1999).

In humans, molecular cloning has identified two receptors for TXA_2, termed TPα and TPβ, which arise by differential splicing and which differ exclusively in their carboxyl terminal (C) tails (Kinsella, 2001). Although both TPα and TPβ exhibit identical G protein-dependent coupling to PLC, the main effector of TP receptor activation, they display differential regulation of their secondary effector adenylyl cyclase and the novel, high-molecular-weight G protein Gh (Walsh et al., 1998; Kinsella, 2001); they exhibit different patterns of expression (Miggin and Kinsella, 1998); and they are subject to differential homologous desensitization (Kinsella, 2001) and heterologous desensitization by a number of other prostanoids, including prostaglandin (PG)I_2, PGE_2, and PGD_2 (Walsh et al., 2000; Walsh and Kinsella, 2000; Kinsella, 2001). In view of these findings highlighting critical differences between the TP isoforms, the aim of the current study was to define the key regulatory elements involved in TXA_2-mediated activation of the ERK signaling cascade and to investigate whether the individual TP receptors may regulate this essential mitogenic cascade. These studies provide the first in-depth study defining the mechanisms of TXA_2-mediated ERK activation through the human TP receptors.

Experimental Procedures

Materials

PD 98059, GF 109203X, Tyrphostin AG1478, PP2, and H-89 were purchased from Calbiochem-Novabiochem (Nottingham, UK). 5-Heptenoic acid, 7-[6-93-hydroxy-1-octenyl-2-oxabicyclo[2.2.1]hept-5-yl]-[1*R*-[1α,4α,5β(z), 6α(1E,3S*)]-9,11-dideoxy-9α,11α-methano epoxy prostaglandin $F_{2\alpha}$ (U46619) and [1*S*-[1α,2β-(5*Z*)-3β,4α-]]-7-[3-[[2-(phenylamino)carbonyl]hydrazine] methyl]-7-oxabicyclo[-2,2,1-]hept-2yl]-5-heptenoic acid (SQ29,548) were purchased from Cayman Chemical (Ann Arbor, MI). [γ^{32}P]ATP (6000 Ci/mmol; 10 mCi/ml) was purchased from PerkinElmer Life Sciences (Boston, MA). Anti-ACTIVE mitogen-activated protein kinase rabbit polyclonal antibody was purchased from Promega (Madison, WI). Chemiluminescence blotting substrate (peroxidase), rat monoclonal 3F10 anti-hemagglutinin (HA)-peroxidase, and β-galactosidase staining kit (#1828-673) were purchased from Roche Applied Science (Sussex, UK). Affinity-purified rabbit polyclonal anti-ERK1 (691); anti-Ha-Ras 259 rat monoclonal antibody (Sc 35); anti-GRK2/β-ARK1 (C15, Sc-562); anti-Rap1B (C-17, Sc 1481); anti-Gβ1(C-16, Sc 379); anti-Gγ2 (A-16, Sc 374); anti-PI3Kγ (H-199; Sc 7177); and horseradish peroxidase-conjugated anti-rabbit, -mouse, or -rat IgG were purchased from Santa Cruz Biotechnology (Santa Cruz, CA). Aprotinin, benzamidine, leupeptin, myelin basic protein (MBP), phorbol-12-myristate-13-acetate (PMA), protein A-Sepharose CL-4B, protein G-agarose, phosphatidylinositol 3-kinase, 2-(4-morpholinyl)-8-phenyl-4*H*-1-benzopyran-4-one (LY294002), epidermal growth factor, and wortmannin were purchased from Sigma Chemical (St. Louis, MO). Anti-HA 101r was purchased from BABCO (Berkeley, CA). I-Block was purchased from Tropix (Bedford, MA). Anti-phosphorylation-specific (pS^{473}) PKB was purchased from BioSource International (Camarillo, CA).

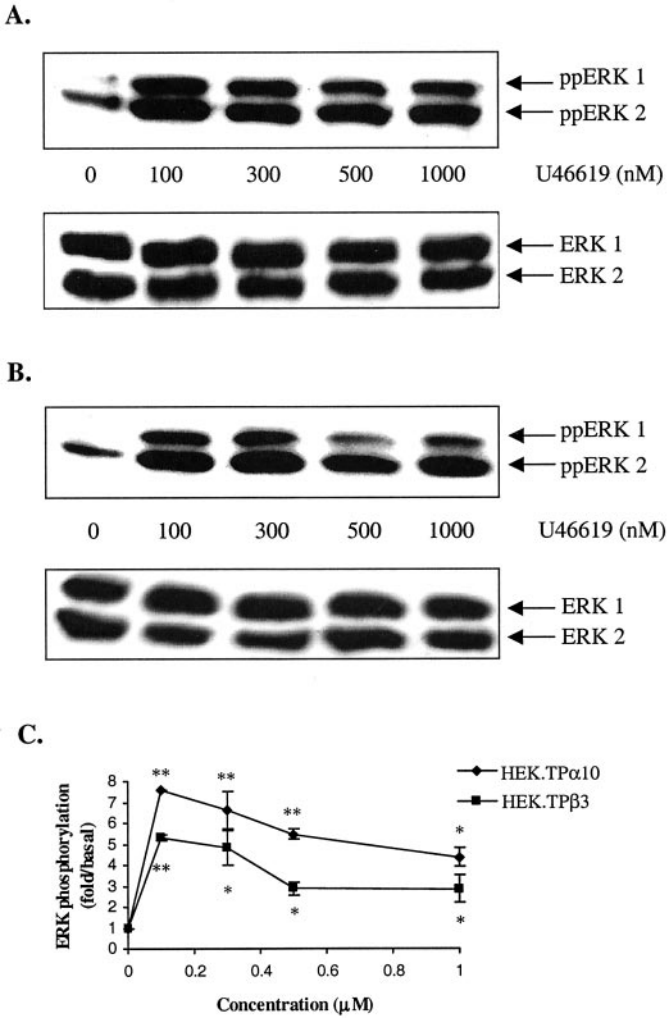

Fig. 1. Concentration-dependent effect of U46619 on ERK1 and ERK2 activation in HEK.TPα10 and HEK.TPβ3 cells. HEK.TPα10 cells (A) or HEK.TPβ3 cells (B) were stimulated for 10 min with 0 to 1000 nM U46619. A and B, blots (top) were screened with anti-ACTIVE-ERK to detect the phosphorylated, active forms of ERK (ppERK1/2), whereas blots (bottom) were screened with anti-ERK antibodies to detect ERK1/2 immunoreactive protein. Results are representative of three independent experiments. C, fold increases in ERK (ppERK1/2) phosphorylation in A (HEK.TPα10 cells) and B (HEK.TPβ3 cells), respectively, are presented as mean fold increases of basal ERK phosphorylation ± S.E.M. ($n = 3$), where the levels of basal ERK phosphorylation in vehicle-treated cells are assigned a value of 1.0. *, $p < 0.05$ and **, $p < 0.01$ indicate that the levels of U46619-mediated ERK activation (ppERK) were significantly greater compared with basal levels.

[^{3}H]SQ29,548 (50.4 Ci/mmol) was obtained from PerkinElmer Life Sciences. All other chemicals and reagents were of AnalaR grade or molecular biology grade and were used without further purification.

Methods

Plasmids. The plasmid pCMV5:Ha-ras has been described previously (Kinsella et al., 1991). The plasmid pCMV5:Ha-ras^{N17} encoding the dominant negative (DN) Ha-Ras^{N17}, whereby Ser^{17} of Ha-Ras was mutated to Asn^{17}, was constructed by site-directed mutagenesis with the QuikChange site-directed mutagenesis kit (Stratagene, La Jolla, CA). The DN [or kinase dead (KD)] plasmids pEF-BOS-c-raf^{KD}-HA^2 (K375W), pEF-BOS-A-raf^{KD}-HA^2 (K336W), pEF-BOSΔRI:Δp85-HA^2 (p85 DN), and the wild-type pEF-BOSΔRI:p85-HA^2, described previously (Sutor et al., 1999), were kindly donated by Dr. Larry M. Karnitz (Division of Radiation Oncology, Mayo Clinic, Rochester, MN). The plasmid pcDNA3:PI3KγDN (K832R) was a generous gift from Dr. Reinhard Wetzker (Max-Planck Research Unit, Jena, Germany). The plasmid pRK5:βARK1(495-689), as described previously (Koch et al., 1994), was a generous gift from Prof. Robert Lefkowitz (Howard Hughes Medical Institute, Duke University Medical Center, Durham, NC). The plasmid pCMVrap1b^{N17}, as described previously (Schmitt and Stork, 2000), was a generous gift from Dr. Philip Stork (Vollum Institute, Oregon Health Sciences University, Portland, OR). The full-length rat Gβ$_1$ and bovine Gγ2 were amplified by reverse transcriptase-polymerase chain reaction followed by subcloning into pcDNA3 (Invitrogen, Carlsbad, CA); the cloned cDNAs were verified by nucleotide sequence analysis and were confirmed to be identical to the previously published sequences for the rat Gβ1 (GenBank accession no. U34958) and bovine Gγ2 (GenBank accession no. M37183) sequences, respectively.

Cell Culture and Transfection. Human embryonic kidney (HEK) 293 cells were obtained from the American Type Culture Collection (Manassas, VA) and were routinely grown in minimal essential medium (MEM), 10% fetal bovine serum (FBS), unless otherwise indicated. The previously described recombinant

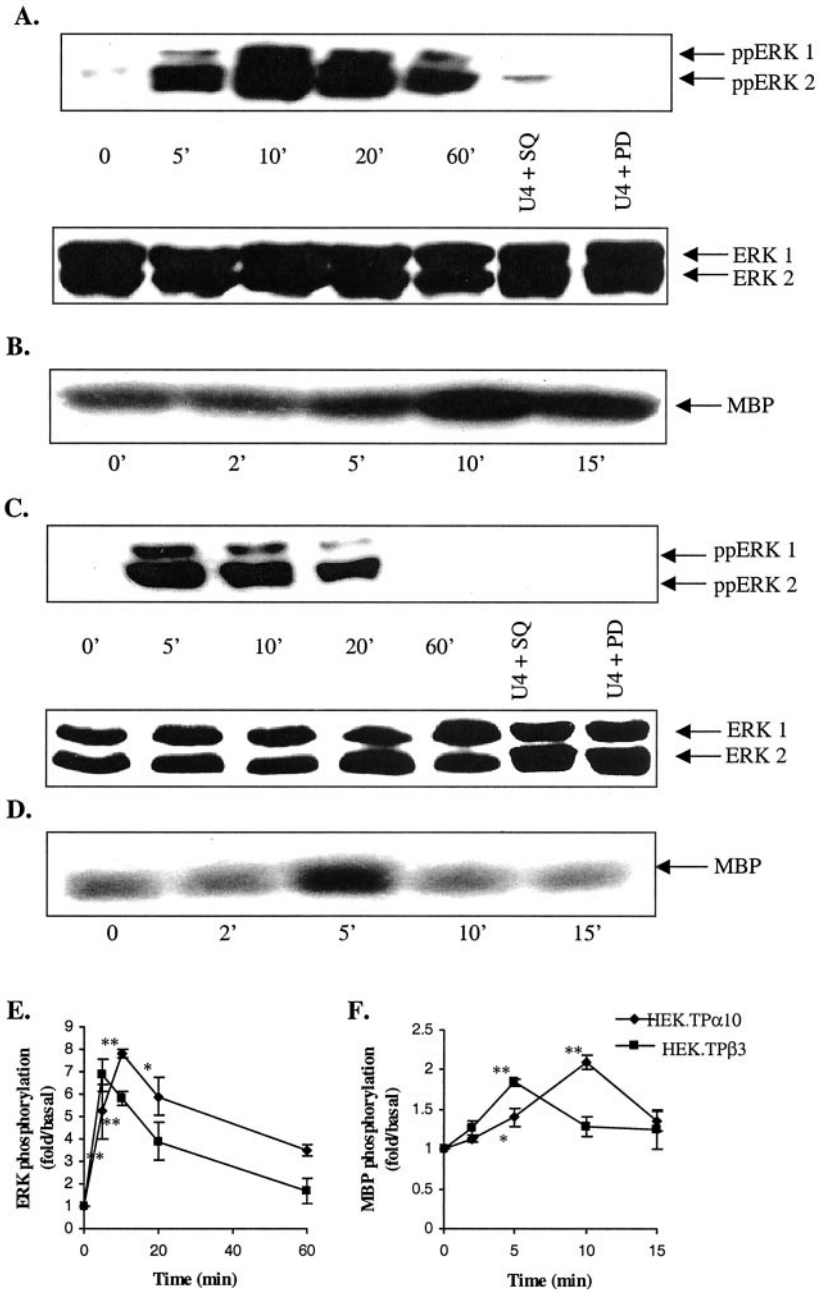

Fig. 2. Time-dependent effect of U46619 on ERK1 and ERK2 activation in HEK.TPα10 and HEK.TPβ3 cells. HEK.TPα10 (A) and HEK.TPβ3 (C) cells were stimulated for 0 to 60 min with 100 nM U46619. Additionally, HEK. TPα10 (A) and HEK.TPβ3 (C) cells were preincubated with SQ29,548 (1 μM; 1 min) or PD 98059 (10 μM; 30 min) before stimulation for 10 min with 100 nM U46619. A and C, blots were screened with anti-ACTIVE-ERK to detect ppERK1/2 (A and C, top) or with anti-ERK antibodies to detect ERK1/2 immunoreactive protein (A and C, bottom). Results are representative of three independent experiments. B and D, HEK.TPα10 cells and HEK.TPβ3 cells, respectively, were stimulated with 100 nM U46619 for 0 to 15 min and U46619-mediated ERK activation was determined using an in vitro kinase assay. Positions of the γ^{32}P-labeled MBP are indicated by the arrow. E, fold increases in ERK (ppERK1/2) phosphorylation in A (HEK.TPα10 cells) and C (HEK.TPβ3 cells), respectively, are presented as mean fold increases of basal ERK phosphorylation ± S.E.M. (n = 3), where the levels of basal ERK phosphorylation in vehicle-treated cells are assigned a value of 1.0. *, $p < 0.05$ and **, $p < 0.01$ indicate that the levels of U46619-mediated ERK activation (ppERK) were significantly greater compared with basal levels. F, fold increases in MBP phosphorylation in B (HEK.TPα10 cells) and D (HEK.TPβ3 cells), respectively, are presented as mean fold increases of basal MBP phosphorylation ± S.E.M. (n = 3), where the levels of basal MBP phosphorylation in vehicle-treated cells are assigned a value of 1.0.

HEK.TPα10 and HEK.TPβ3 cell lines, stably overexpressing TPα and TPβ, respectively (Walsh et al., 1998, 2000), were routinely grown in MEM, 10% FBS unless otherwise indicated. For transient transfections, HEK.TPα10 and HEK.TPβ3 cells were plated in 10-cm culture dishes 24 h before transfection at a density of 2×10^6 cells/10-cm dish in MEM, 10% FBS. Cells were cotransfected with 25 μg of pCMV5-, pcDNA3-, or pEF-BOS-based vectors, or as negative controls, with 25 μg of the appropriate empty vector, either pCMV5 or pcDNA3, plus 10 μg of pADVA by using the calcium phosphate/DNA coprecipitation technique (Walsh et al., 1998). HEK 293 cells transiently transfected in this way were routinely harvested 48 h post-transfection. However, for the measurement of mitogenic responses, 48 h post-transfection the complete medium (MEM, 10% FBS) was replaced with serum-free medium (MEM, 0% FBS) and the cells were incubated for a further 48 h to induce quiescence. In all cases, transient expression of proteins was confirmed by Western blot analysis at 48 to 96 h post-transfection. Specifically, expression of Ha-Ras and Ha-Ras^{N17} was confirmed by immunoblot analysis with anti-Ha-Ras (Sc-35); expression of HA-tagged c-Raf, A-Raf, and p85^{DN} were confirmed using the anti-HA 3F10 peroxidase conjugate; expression of Rap1b^{N17} was confirmed using an anti-Rap1B (Sc 1481); expression of βARK1(495-689) was confirmed using anti-GRK 2 (Sc-562); expression of PI3Kγ was established using anti-PI3Kγ (Sc 7177) antibody; and expression Gβ1 and Gγ2 were confirmed using the anti-Gβ1 (Sc 379) and anti-Gγ2 (Sc 374) antisera, respectively.

Saturation Radioligand Binding. Radioligand binding was performed essentially as described previously (Miggin and Kinsella, 1998). Briefly, HEK 293 cells transiently transfected with pCMV5:TPα were harvested by centrifugation at 500*g* at 4°C for 5 min and then washed three times in phosphate-buffered saline (PBS). Protein concentrations were determined using the Bradford assay (Miggin and Kinsella, 1998). Cells were then harvested and resuspended in modified Ca^{2+}/Mg^{2+}-free Hanks' buffered salt solution, containing 10 mM HEPES, pH 7.67, 0.1% bovine serum albumin at a final concentration of 1 mg/ml. Saturation radioligand binding experiments with the TP antagonist [^{3}H]SQ29,548 (20 nM; 50.4 Ci/mmol) were carried out at 30°C for 30 min in 100-μl reactions by using approximately 100 μg of total cellular protein per assay. Nonspecific binding was determined in the presence of excess nonlabeled 10 μM SQ29,548. Reactions were terminated by the addition of ice-cold 10 mM Tris, pH 7.4, followed by filtration through Whatman GF/C glass filters (Whatman, Maidstone, UK). After washing of the filters three times with 4 ml of 10 mM Tris, pH 7.4, liquid scintillation counting of the filters in 5 ml of scintillation cocktail was performed. Results are expressed as picomoles of [^{3}H]SQ29,548 incorporated per milligram of cell protein ± S.E.M., where $n = 3$.

β-Galactosidase Staining. Briefly, HEK 293 cells were transiently transfected with pHM6:lacZ (Roche Applied Science) by using the calcium phosphate/DNA coprecipitation technique (Walsh et al., 1998). After 48 and 96 h, β-galactosidase activity was assessed using the β-galactosidase staining kit, essentially as described by the manufacturer (Roche Applied Science). Briefly, cells were washed once with PBS. After removal of the PBS, the cells were fixed with PBS containing 2% formaldehyde (3 ml/10-cm dish) for 15 min at room temperature. Cells were washed three times with PBS followed by analysis of β-galactosidase activity with a staining solution (1 part X-gal:19 parts iron buffer). After incubation of the cells for 60 min at 37°C, 5% CO_2, stained and nonstained cells were counted in a num-

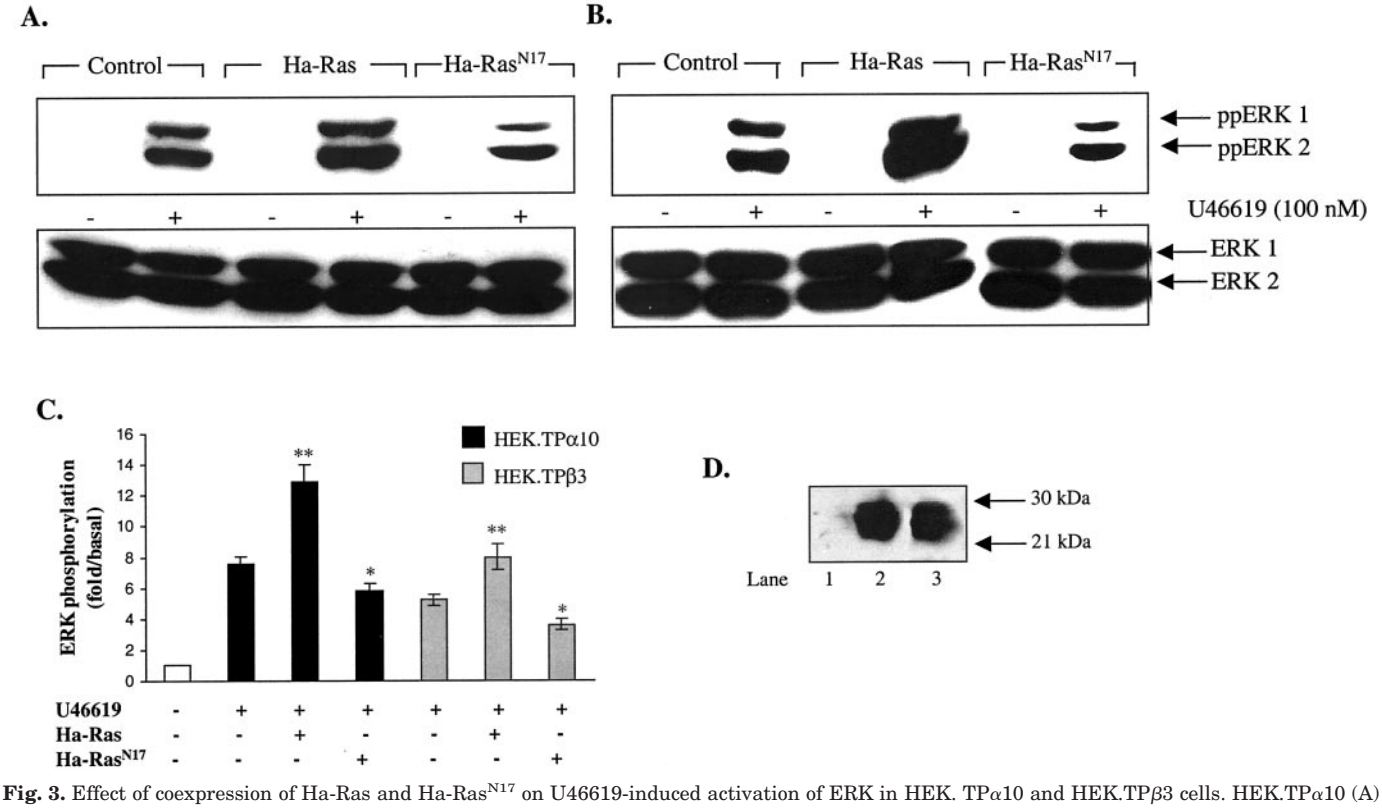

Fig. 3. Effect of coexpression of Ha-Ras and Ha-Ras^{N17} on U46619-induced activation of ERK in HEK. TPα10 and HEK.TPβ3 cells. HEK.TPα10 (A) and HEK.TPβ3 (B) were transiently transfected with either pCMV5:Ha-Ras, pCMV5:Ha-RasN17, or as a control, with the vector pCMV5. Cells were stimulated with U46619 for 10 min (+), with cells exposed to vehicle alone (−) serving as references. A and B, blots were screened with anti-ACTIVE-ERK to detect ppERK1/2 (A and B, top) or with anti-ERK antibodies to detect ERK1/2 immunoreactive protein (A and B, bottom). Results are representative of four independent experiments. C, fold increases in ERK phosphorylation (ppERK1/2) in A and B are presented as mean fold increases of basal ERK phosphorylation ± S.E.M. ($n = 4$), where the levels of basal ERK phosphorylation in vehicle-treated cells (−) are assigned a value of 1.0. *, $p < 0.05$ and **, $p < 0.01$ indicate that the levels of U46619-mediated ppERK activation were significantly enhanced/reduced in the presence of Ha-ras and Ha-ras^{N17}, respectively. D, immunoblot analysis of total cellular protein (100 μg) by using anti-Ha-Ras antibody (259; Santa Cruz Biotechnology) to confirm expression of Ha-Ras (lane 2) and Ha-Ras^{N17} (lane 3) with HEK 293 cells serving as a reference (lane 1).

ber of random fields of the dish. Transfection efficiency was determined as mean percentage (%) of stained cells per total cell population ± S.E.M., where $n = 3$.

Determination of ERK Activity by Using an in Vitro Kinase Assay. HEK.TPα10 and HEK.TPβ3 cells were seeded at 4×10^5 cells/60-mm dish in MEM, 10% FBS. After 24 h, cells were exposed to MEM, 0.5% FBS to induce quiescence. After a further 48 h, the cells were exposed to test agents for the appropriate times, as indicated in the respective figure legends. ERK activity was determined by monitoring ERK-mediated phosphorylation of its substrate myelin basic protein as described previously (Coso et al., 1995; Miggin and Kinsella, 2001).

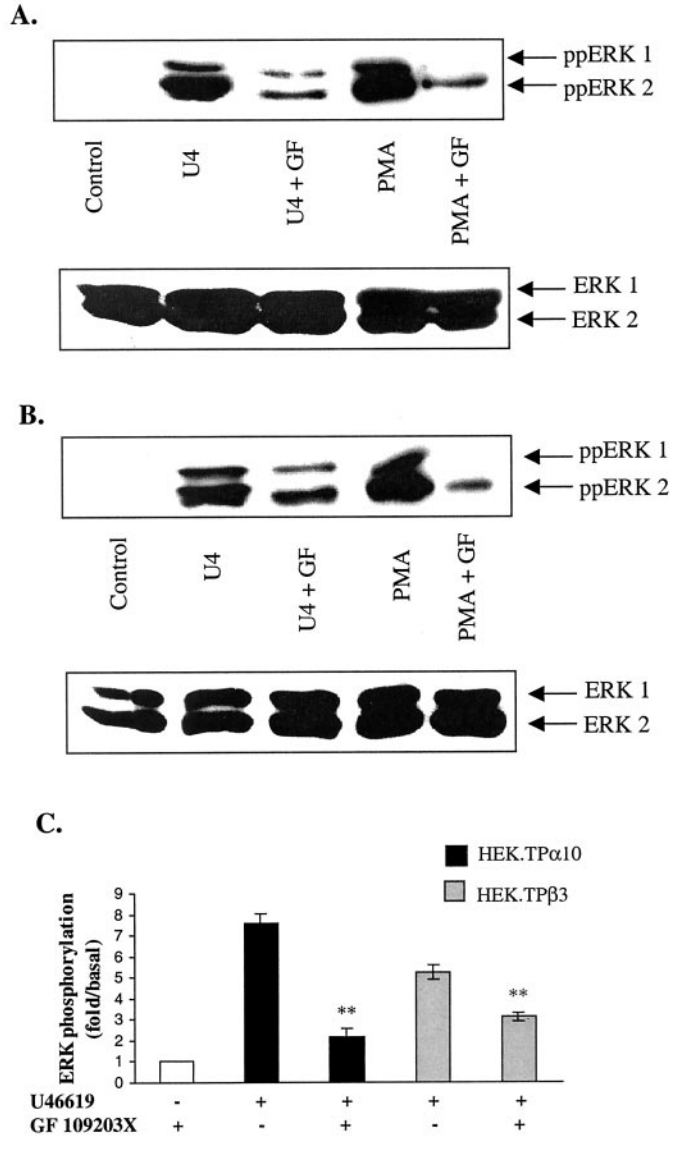

Fig. 4. Effect of GF 109203X on U46619-induced activation of ERK1 and ERK2 in HEK.TPα10 and HEK.TPβ3 cells. HEK.TPα10 (A) and HEK.TPβ3 (B) cells were preincubated with GF 109203X (GF; 500 nM; 30 min). Subsequently, U46619 (U4; 100 nM) or PMA (250 nM; 20 min) was added for 10 min, with cells exposed to U46619 alone (100 nM; 10 min), PMA alone (250 nM; 20 min), or vehicle alone (Control) serving as references. A and B, blots were screened with anti-ACTIVE-ERK to detect ppERK1/2 (A and B, top) or with anti-ERK antibodies to detect ERK1/2 immunoreactive protein (A and B, bottom). Results are representative of six to eight independent experiments. C, fold increases in ERK phosphorylation (ppERK1/2) in A and B are presented as mean fold increases of basal ERK phosphorylation ± S.E.M. ($n = 8$), where the levels of basal ERK phosphorylation in vehicle-treated cells (−) are assigned a value of 1.0. **, $p \leq 0.01$ indicates that the levels of U46619-induced ppERK activation were significantly reduced in the presence of GF 109203X.

Determination of ERK/PKB Activation by Immunoblot Analysis. HEK.TPα10 and HEK.TPβ3 cells were seeded at 1.5×10^6 cells/10-cm dish in MEM, 10% FBS. After 24 h, cells were exposed to MEM, 0% FBS to induce quiescence. After 48 h, the cells were exposed to test compounds, as indicated in the respective figure legends. Cellular lysates were prepared as described previously (Boulton et al., 1991). Aliquots (30 μg) of the resultant supernatant were subjected to 12.5% SDS-polyacrylamide gel electrophoresis followed by electroblotting onto PVDF membranes. Thereafter, membranes were screened by immunoblot analysis with a rabbit anti-ACTIVE ERK antibody (Promega) or a rabbit anti-phosphorylated PKB/Akt antibody (BioSource) as appropriate, to detect dual phosphorylated ERK (ppERK) and phosphorylated S^{473}PKB (ppPKB), respectively, essentially as recommended by the supplier. Where appropriate, membranes were rescreened with an affinity-purified rabbit anti-ERK antibody (Santa Cruz Biotechnology) to detect total ERK protein. Immunocomplexes were visualized using the chemiluminescence detection system, as described by the supplier (Roche Applied Science); signals were quantified by scanning densitometry with a UVP gel documentation system. Results presented are representative of at least three independent experiments. Alternatively, signals from ppERK1 and ppERK2 (combined signals) or ppPKB were quantified by densitometry with a UVP gel documentation system and the combined ppERK1/2 or ppPKB signals are presented as mean fold increase of basal ERK/PKB phosphorylation ± S.E.M., where the levels of basal ERK/PKB phosphorylation in vehicle-treated cells are assigned a value of 1.0. During densitometric analyses, the signals from ppERK1 and ppERK2 were combined because the ratio of ppERK1/ppERK2 was constant. Statistical analyses were performed using the unpaired Students' t test with the Statworks analysis package. p values ≤ 0.05 indicate a statistically significant difference.

Coimmunoprecipitation of p85 with TPα and TPβ. HEK.TPα10 and HEK.TPβ3 cells were transiently transfected with pEF-BOSΔRI:Δp85-HA[2] and pADVA by using the Effectene transfection reagent essentially as described by the manufacturer (QIAGEN, Valencia, CA). After 48 h, cells were stimulated with U46619 (100 nM; 10 min) with nonstimulated cells serving as a reference. After harvesting, aliquots (80 μg) of whole cell protein were resolved by SDS-PAGE and electroblotted onto PVDF membranes. For immunoprecipitations, whole cell protein (500 μg) from each transfection was immunoprecipitated using the anti-TPα (1/100) and anti-TPβ (1/100) antisera directed to peptide sequences unique to TPα (amino acid residues SLSLQPQLTQRSGLQ; α peptide) and TPβ (amino acid residues LPFEPPTGKALSRKD; β peptide) C-tail sequences, as described previously (Miggin and Kinsella, 2001). Alternatively, as negative controls, whole cell protein (500 μg) from each transfection was subjected to immunoprecipitation by using the control preimmune TPα (1/100) and TPβ (1/100) sera. Immunoprecipitations were carried out essentially as described previously (Walsh et al., 2000; Miggin and Kinsella, 2001). Briefly, cells were washed once with ice-cold phosphate-buffered saline (3 ml/dish) and were then lysed with 0.6 ml of radioimmune precipitation buffer [50 mM Tris-Cl, pH 8.0, 150 mM NaCl, 1 mM EDTA, 1% Nonidet P-40 (v/v), 0.5% sodium deoxycholate (w/v), 0.1% SDS (w/v) containing 10 mM sodium fluoride, 25 mM sodium pyrophosphate, 1 μg/ml leupeptin, 0.5 mM phenylmethylsulfonyl fluoride, 10 μg/ml aprotinin, 10 μg/ml antipain, and 1 mM sodium orthovanadate]. After incubation on ice for 15 min, cells were harvested and disrupted by sequentially passing through hypodermic needles of decreasing bore size (gauge 20, 23, and 26), and soluble lysates were harvested by centrifugation at 13,000g at room temperature for 5 min. Coimmunoprecipitation of TPα and TPβ receptors from the cell lysates was performed using either anti-TPα (1/100) or anti-TPβ (1/100) antisera as appropri-

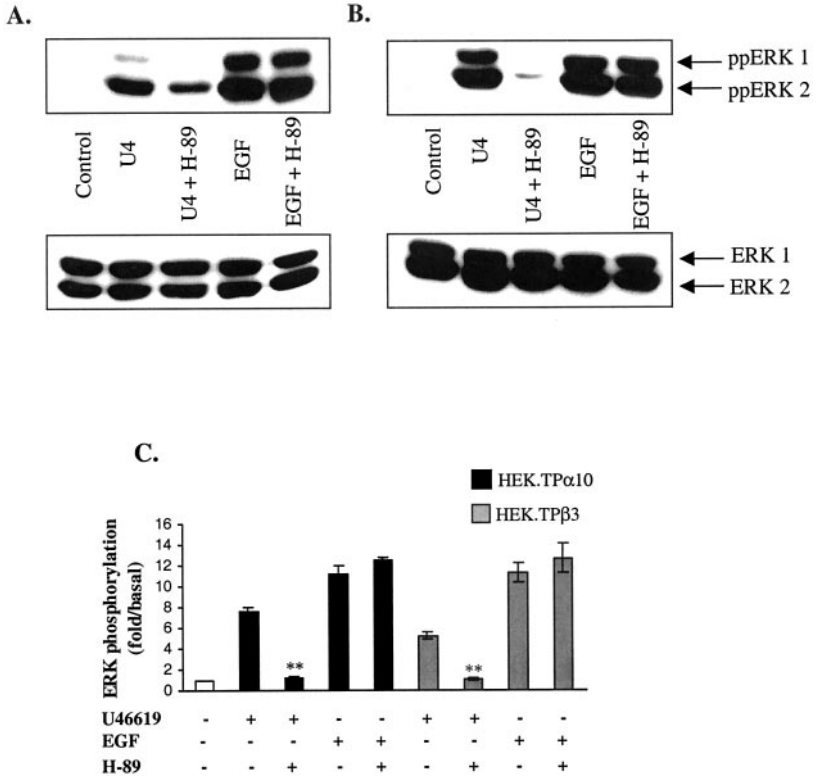

Fig. 5. Effect of H-89 on U46619-induced activation of ERK1 and ERK2 in HEK.TPα10 and HEK.TPβ3 cells. HEK.TPα10 (A) and HEK.TPβ3 (B) cells were preincubated for 5 min in the absence or presence of 10 μM H-89 before stimulation for 10 min with 100 nM U46619, 10 ng/ml EGF with cells exposed to vehicle alone serving as references. A and B, blots were screened with anti-ACTIVE-ERK to detect ppERK1/2 (A and B, top) or with anti-ERK antibodies to detect ERK1/2 immunoreactive protein (A and B, bottom). Results are representative of four independent experiments. C, fold increases in ERK phosphorylation (ppERK1/2) in A and B are presented as mean fold increases of basal ERK phosphorylation ± S.E.M. (n = 4), where the levels of basal ERK phosphorylation in vehicle-treated cells (−) are assigned a value of 1.0. **, indicates that the levels of U46619-mediated ppERK activation were significantly reduced in the presence ($p \leq 0.01$) of H-89.

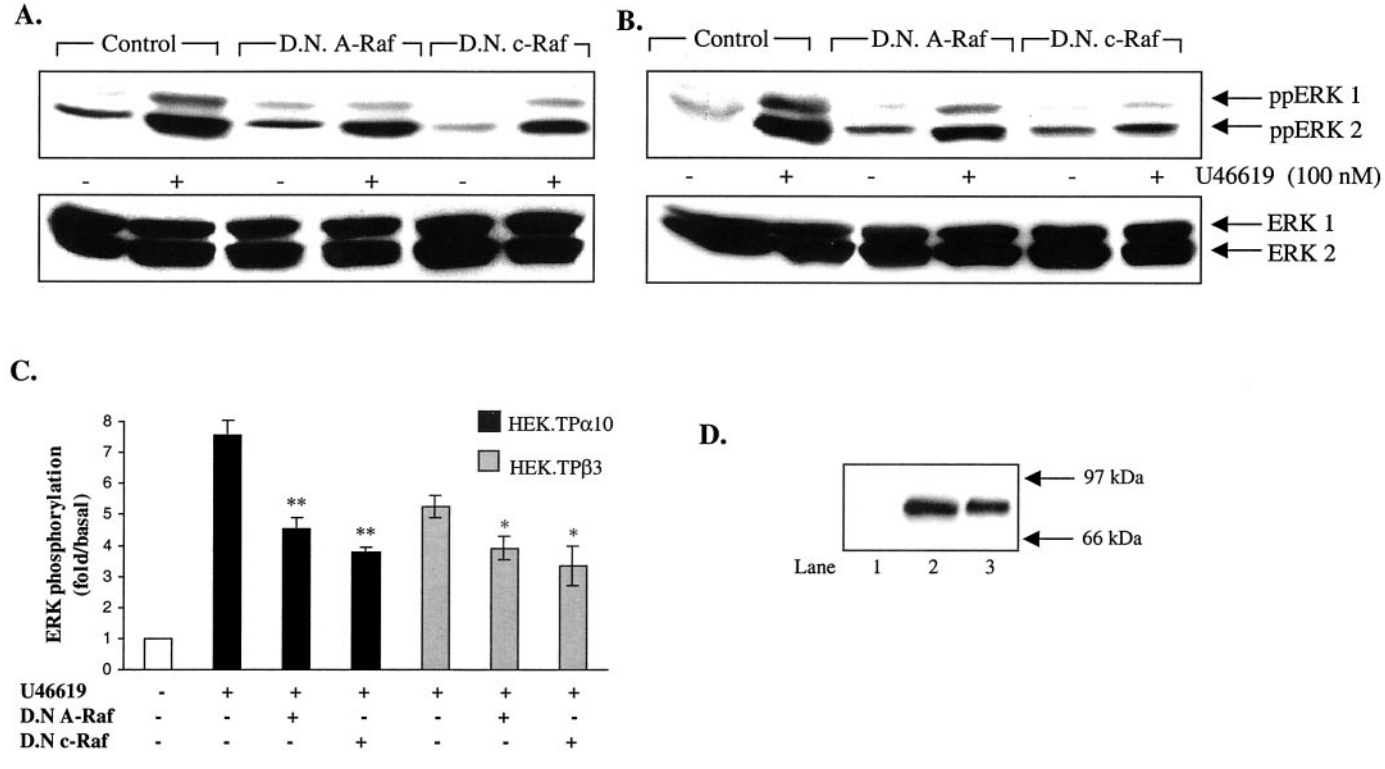

Fig. 6. Effect of coexpression of DN A-Raf and DN c-Raf on U46619-induced ERK activation in HEK. TPα10 and HEK.TPβ3 cells. HEK.TPα10 (A) and HEK.TPβ3 (B) were transiently transfected with either pEF-BOS:A-Raf.HA^2 DN (DN A-Raf) or pEF-BOS:c-Raf.HA^2 DN (DN c-Raf) or the empty vector (Control). Cells were stimulated with U46619 for 10 min (+), with cells exposed to vehicle alone (−) serving as references. A and B, blots were screened with anti-ACTIVE-ERK to detect ppERK1/2 (A and B, top) or with anti-ERK antibodies to detect ERK1/2 immunoreactive protein (A and B, bottom). Results are representative of four independent experiments. C, fold increases in ERK phosphorylation (ppERK1/2) in A and B are presented as mean fold increases of basal ERK phosphorylation ± S.E.M. (n = 4), where the levels of basal ERK phosphorylation in vehicle-treated cells (−) are assigned a value of 1.0. *, $p \leq 0.05$ and **, $p \leq 0.01$ indicate that the levels of U46619-mediated ppERK activation were significantly reduced in the presence of DN A-Raf and c-Raf. D, immunoblot analysis of total cellular lysate (30 μg) to confirm expression of c-Raf (lane 2) and A-Raf (lane 3) with nontransfected HEK 293 cells serving as a reference (lane 1).

ate. Immunoprecipitates were resolved by SDS-PAGE followed by electroblotting onto PVDF membranes. Thereafter, membranes were screened by immunoblot analysis by using either the anti-HA 3F10 peroxidase conjugate (to detect coimmunoprecipitation of HA-tagged p85 with TPα and TPβ) or by using the anti-HA-101r (BABCO) followed by peroxidase-conjugated anti-mouse IgG (to detect HA-tagged p85 cellular protein). To confirm the specificity of the anti-TPα and anti-TPβ antisera to immunoprecipitate TPα and TPβ, the previously described cell lines HEK-.HATPα and HEK.HATPβ were used (Walsh et al., 2000). Both HA-tagged TPα and HA-tagged TPβ were subjected to immunoprecipitation by using the anti-TPα antisera (1/100), anti-TPβ (1/100), or anti-HA 101r (1/300; BABCO) antisera as described previously (Walsh et al., 2000) with HEK 293 cells serving as a control. Immunoprecipitates were resolved by SDS-PAGE followed by electroblotting onto PVDF membranes. Thereafter, membranes were screened by immunoblot analysis by using the anti-HA 3F10 peroxidase conjugate (to detect immunoprecipitation of HA-tagged TPα and TPβ).

Results

U46619-Mediated ERK Activation in HEK.TPα10 and HEK.TPβ3 Cells. Maximal concentration-dependent activation of ERK1 and ERK2 occurred in HEK.TPα10 cells after their exposure to 100 nM U46619 (Fig. 1, A and C). In HEK.TPβ3 cells, maximal ERK1/2 activation occurred after their exposure to 100 to 300 nM U46619 (Fig. 1, B and C).

Exposure of HEK.TPα10 (Fig. 2, A and E) and HEK.TPβ3 (Fig. 2, C and E) cells to U46619 induced time-dependent ERK1/2 activation with maximal responses observed at 10 min in HEK.TPα10 cells and at 5 min in HEK.TPβ3 cells, respectively. ERK activation was also determined using an in vitro kinase reaction with MBP serving as an ERK phosphorylation substrate. U46619 induced a time-dependent activation of ERK in HEK.TPα10 cells and in HEK.TPβ3 cells with maximal MBP phosphorylation observed after 10 min (Fig. 2, B and F) and after 5 min (Fig. 2, D and F), respectively. The

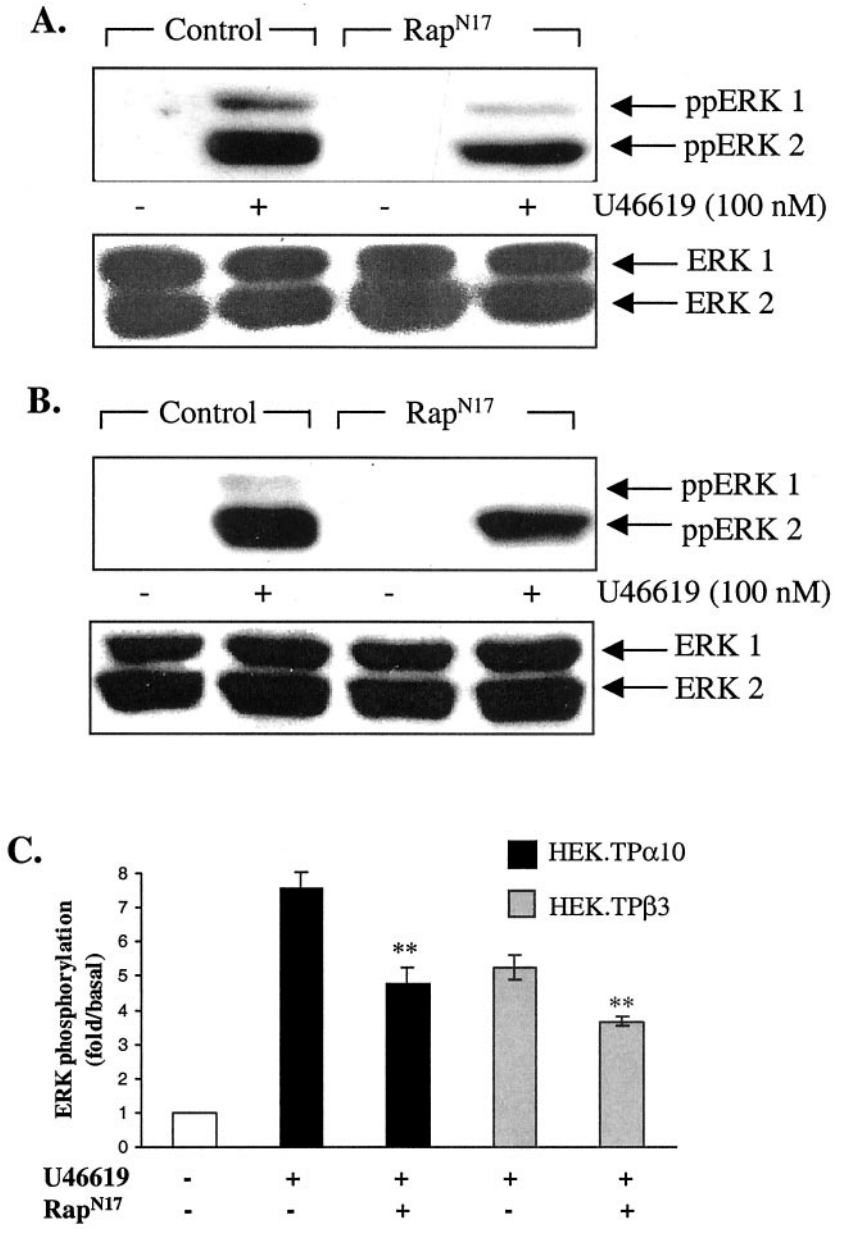

Fig. 7. Effect of coexpression of Rap1b^{N17} on U46619-induced ERK activation in HEK.TPα10 and HEK.TPβ3 cells. HEK.TPα10 (A) and HEK.TPβ3 (B) were transiently transfected with pCMV:Rap1b^{N17} (Rap^{N17}) or with pCMV (Control). Cells were stimulated with U46619 for 10 min (+), with cells exposed to vehicle alone (−) serving as references. A and B, blots were screened with anti-ACTIVE-ERK to detect ppERK1/2 (A and B, top) or with anti-ERK antibodies to detect ERK1/2 immunoreactive protein (A and B, bottom). Results are representative of four independent experiments. C, fold increases in ERK phosphorylation (ppERK1/2) in A and B are presented as mean fold increases of basal ERK phosphorylation ± S.E.M. (n = 4), where the levels of basal ERK phosphorylation in vehicle-treated cells (−) are assigned a value of 1.0. **, $p \leq 0.01$ indicates that the levels of U46619-mediated ppERK activation were significantly reduced in the presence of Rap1b^{N17}.

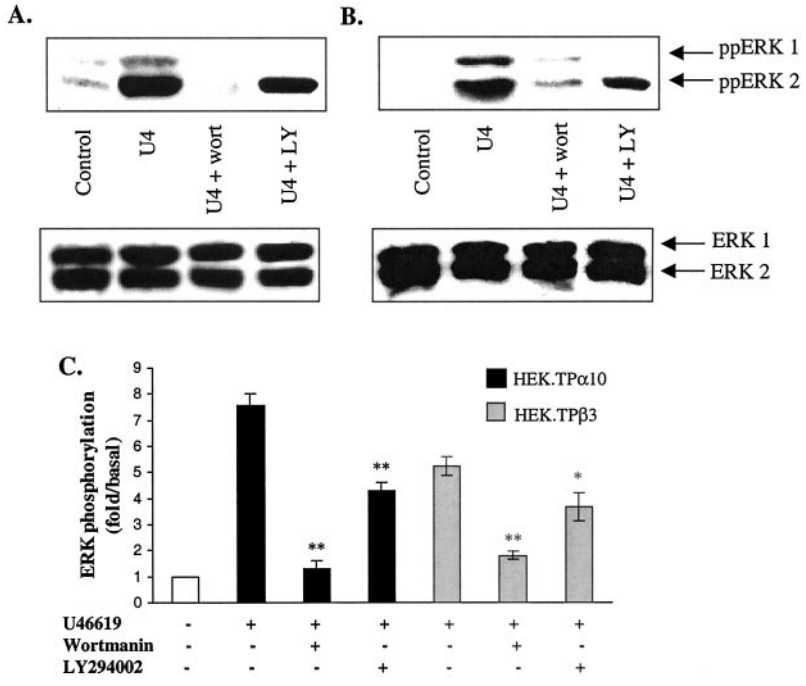

Fig. 8. Effect of wortmannin and LY294002 on U46619-induced activation of ERK1 and ERK2 in HEK.TPα10 and HEK.TPβ3 cells. HEK.TPα10 (A) and HEK.TPβ3 (B) cells were preincubated with either wortmannin (wort; 400 nM; 30 min) or LY294002 (LY; 50 μM; 30 min). Subsequently, the medium was supplemented with U46619 (U4; 100 nM; 10 min), with cells exposed exclusively to U46619 or vehicle alone (Control) serving as references. A and B, blots were screened with anti ACTIVE-ERK to detect ppERK1/2 (A and B, top) or with anti-ERK antibodies to detect ERK1/2 immunoreactive protein (A and B, bottom). Results are representative of four independent experiments. C, fold increases in ERK phosphorylation (ppERK1/2) in A and B are presented as mean fold increases of basal ERK phosphorylation $\pm$ S.E.M. ($n = 4$), where the levels of basal ERK phosphorylation in vehicle-treated cells ($-$) are assigned a value of 1.0. $*$, $p \leq 0.05$ and $**$, $p \leq 0.01$ indicate that the levels of U46619-mediated ppERK activation were significantly reduced in the presence of wortmannin and LY294002.

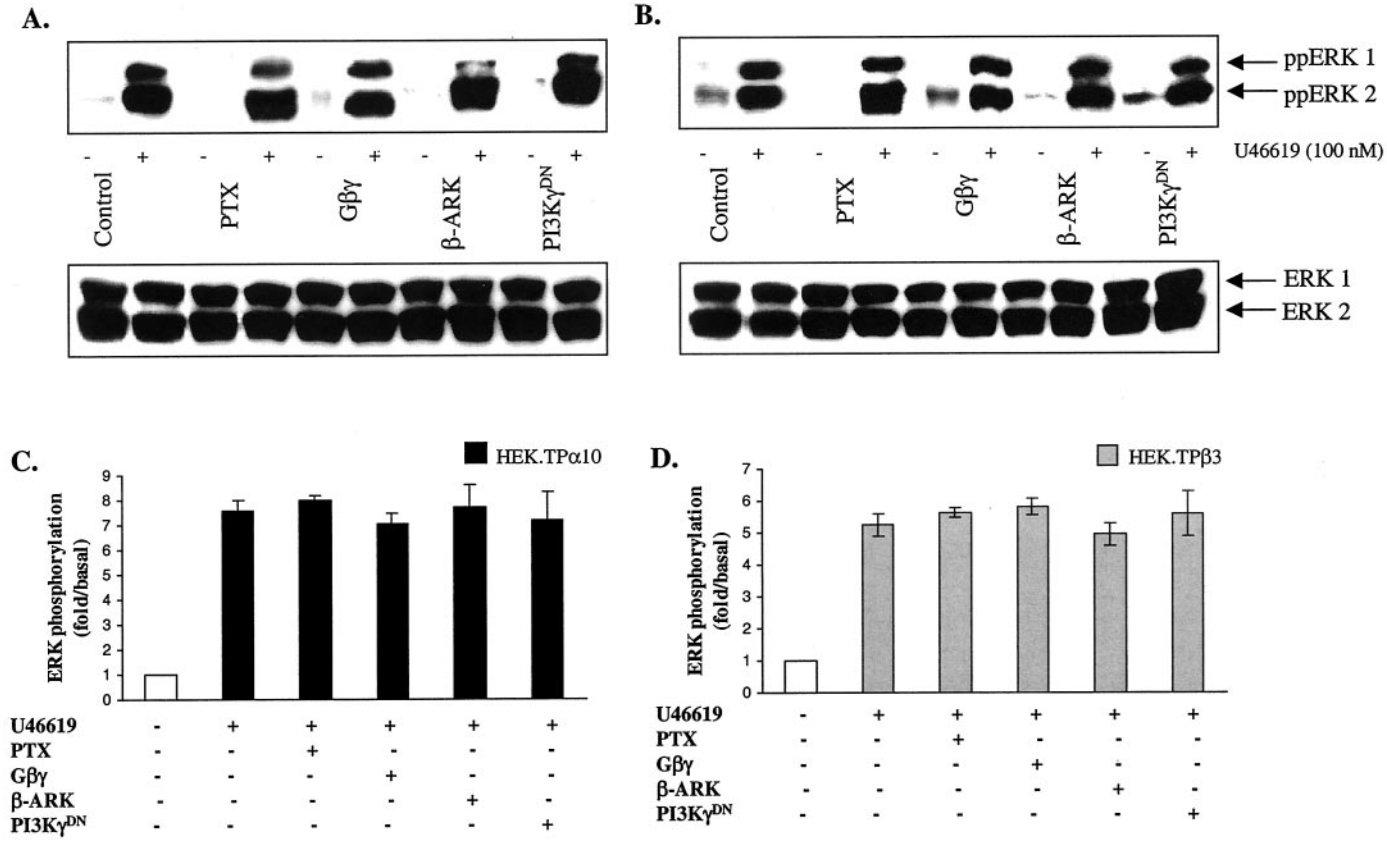

Fig. 9. Role of class I_B PI3Ks on U46619-induced activation of ERK in HEK.TPα10 and HEK.TPβ3 cells. HEK. TPα10 (A) and HEK.TPβ3 (B) cells were transiently transfected with either pcDNA3:Gβ1 plus pcDNA3:Gγ2 (G$\beta\gamma$), pRK5:βARK1(495-689) minigene (β-ARK), pcDNA3:PI3Kγ^{DN} (PI3Kγ^{DN}), or with the vector pcDNA3 (Control). In addition, cells were preincubated with PTx (50 ng/ml; 16 h). Subsequently, cells were stimulated for 10 min with 100 nM U46619 ($+$), with cells exposed exclusively to U46619 or vehicle alone ($-$) serving as a reference. A and B, blots were screened with anti-ACTIVE-ERK to detect ppERK1/2 (A and B, top) or with anti-ERK antibodies to detect ERK1/2 immunoreactive protein (A and B, bottom). Results are representative of four independent experiments. C and D, fold increases in ERK phosphorylation (ppERK1/2) in A and B, respectively, are presented as mean fold increases of basal ERK phosphorylation $\pm$ S.E.M. ($n = 4$), where the levels of basal ERK phosphorylation in vehicle-treated cells ($-$) are assigned a value of 1.0. The levels of U46619-mediated ppERK activation were not significantly altered in the presence of PTX, G$\beta\gamma$, β-ARK, or PI3Kγ^{DN}.

specificity of U46619-induced ERK1/2 activation was confirmed whereby both the selective TP antagonist SQ29,548 and the mitogen-activated protein kinase kinase 1/2 inhibitor PD 98059 abolished ERK activation (ppERK1/2; Fig. 2, A and C) and MBP phosphorylation (data not shown) in both in HEK.TPα10 and HEK.TPβ3 cells. In all cases, equal protein loading and ERK1 and ERK2 expression was confirmed using an anti-ERK antibody to detect total ERK protein expression (Figs. 1, A and B; 2, A and C, bottom).

Thereafter, to determine the role of various protein mediators, such as Ras or PI3K isozymes, in U46619/TXA_2-induced ERK signaling, HEK.TPα10 cells and HEK.TPβ3 cells were transiently cotransfected with cDNAs encoding either wild-type or dominant negative forms of those mediators. To establish the efficiency of transfection and to confirm sustained protein expression at 48 to 96 h post-transfection, for each independent experiment, HEK 293 cells were transfected with the vector pCMV5:TPα and TP expression was determined by saturation radioligand binding analysis with [^{3}H]SQ29,548 at 48 and 96 h post-transfection. Routinely, TPα expression was 1.98 $\pm$ 0.14 and 1.57 $\pm$ 0.12 pmol of [^{3}H]SQ29,548/mg of cell protein after 48 and 96 h post-transfection, respectively. Thus, no significant reduction in TPα protein expression occurred at 96 h post-transfection compared with TPα expression at 48 h ($p = 0.1259$). As an additional control, to determine the efficiency of transfection, HEK 293 cells were transfected with the expression vector pHM6:lacZ. At 48 and 96 h post-transfection, β-galactosidase activity was quantified. Routinely, by using the calcium phosphate/DNA coprecipitation technique, 35 to 40% and 30 to 35% cells expressed β-galactosidase activity at 48 and 96 h post-transfection, respectively.

To investigate the role of Ha-Ras in TP-mediated ERK activation, the effect of overexpression of Ha-Ras and its dominant negative Ha-Ras^{N17} (Schmitt and Stork, 2000) were investigated. Overexpression of Ha-Ras and Ha-Ras^{N17} was confirmed by Western blot analyses (Fig. 3D). Coexpression of Ha-Ras augmented U46619-induced ERK1/2 activation in both HEK.TPα10 and HEK.TPβ3 cells compared with control (pCMV5-transfected) cells (Fig. 3, A–C), whereas Ha-Ras^{N17} significantly reduced U46619-induced ERK1/2 activation in both cell types (Fig. 3, A–C). Furthermore, overexpression of Ha-Ras or Ha-Ras^{N17} in HEK.TPα10 and HEK.TPβ3 cells neither elicited ERK activation in the absence of U46619 (Fig. 3, A–C) nor affected the overall level of TP expression compared with nontransfected cells (data not shown).

Preincubation of HEK.TPα10 and HEK.TPβ3 cells with the EGF receptor inhibitor AG1478 (125 nM; 30 min) or the src inhibitor PP2 (100 nM; 15 min) significantly inhibited U46619-mediated ERK1/2 activation. Specifically, in HEK.TPα10 cells, 7.57 $\pm$ 0.45-, 4.22 $\pm$ 0.06- ($p < 0.01$), and 3.61 $\pm$ 0.15 ($p < 0.01$)-fold increases in U46619-mediated ERK activation over basal levels were observed in the ab-

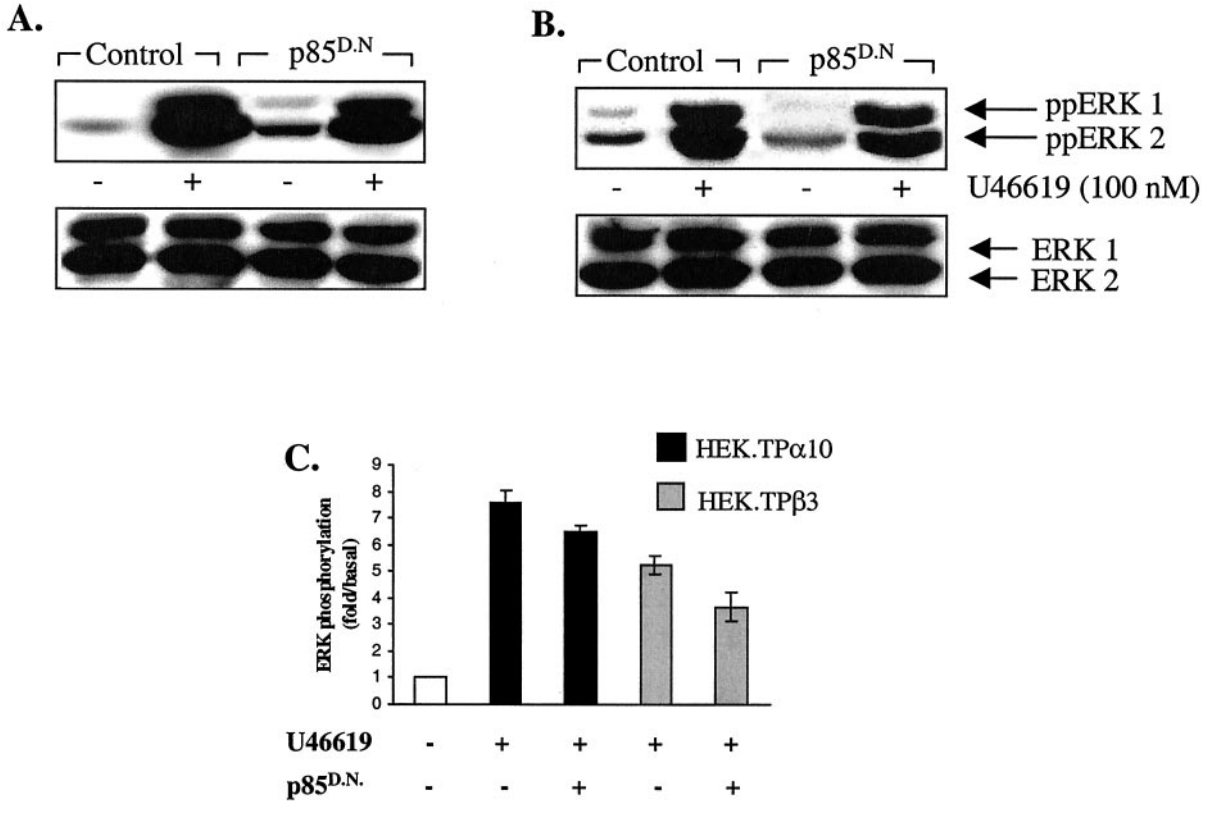

Fig. 10. Effect of dominant negative p85 adaptor subunit of PI3K on TPα- and TPβ-mediated ERK activation. HEK. TPα10 (A) and HEK.TPβ3 (B) cells were transiently transfected with pEF-BOSΔRI:Δp85. HA[2] (p85^{DN}) or with the empty vector (Control). Cells were stimulated with 100 nM U46619 for 10 min (+), with cells exposed to vehicle alone (−) serving as references. A and B, blots were screened with *anti*-ACTIVE-ERK to detect ppERK1/2 (A and B, top) or with anti-ERK antibodies to detect ERK1/2 immunoreactive protein (A and B, bottom). Results are representative of four independent experiments. C, fold increases in ERK phosphorylation (ppERK1/2) in A (HEK.TPα10) and B (HEK.TPβ3), respectively, are presented as mean fold increases of basal ERK phosphorylation $\pm$ S.E.M. ($n = 4$), where the levels of basal ERK phosphorylation in vehicle-treated cells (−) are assigned a value of 1.0.

sence and presence of either AG1478 or PP2, respectively. In HEK.TPβ3 cells, 5.25 ± 0.36-, 2.23 ± 0.28- ($p < 0.005$), and 2.91 ± 0.63 ($p < 0.05$)-fold increases in U46619-mediated ERK activation over basal levels were observed in the absence and presence of either AG1478 or PP2, respectively.

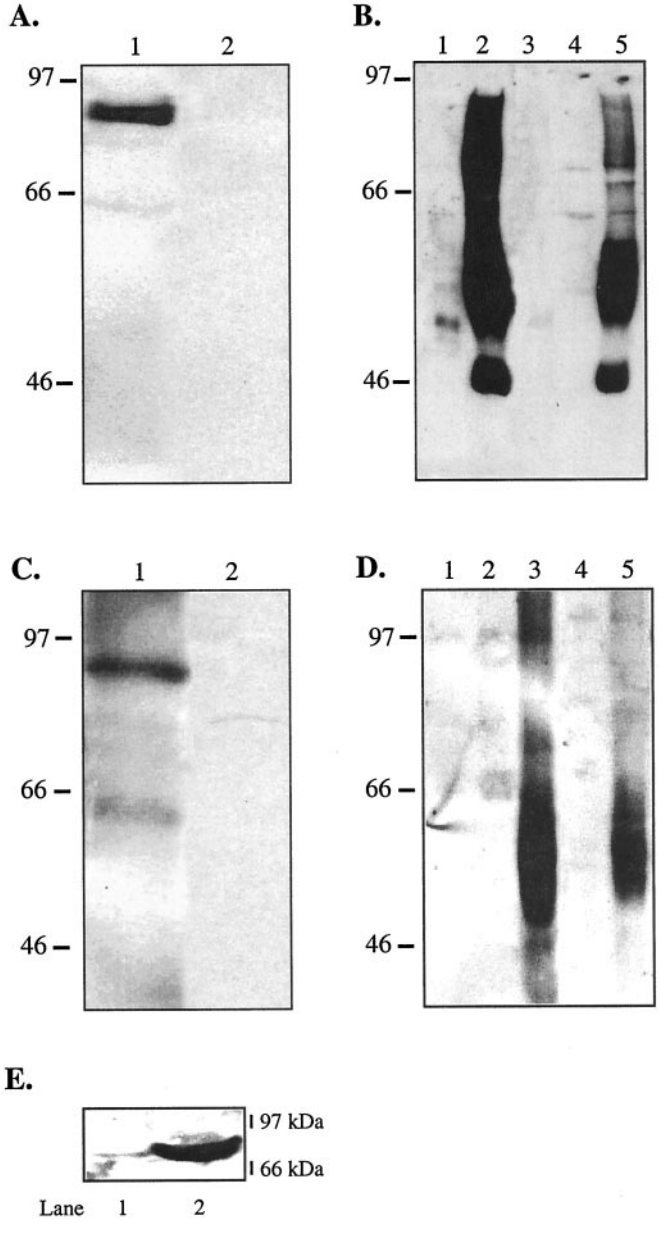

Fig. 11. Association of the p85 adaptor subunit of PI3K with TPα and TPβ.HEK. TPα10 (A) and HEK.TPβ3 (C) cells were transiently transfected with pEF-BOSΔRI:Δp85.HA^2 (p85^{DN}). Cells were stimulated with 100 nM U46619 for 10 min before immunoprecipitation of TPα and TPβ with anti-TPα (A, lane 1) and anti-TPβ (C, lane 1) antisera, respectively, or as negative controls, with the preimmune TPα (A, lane 2) and TPβ (C, lane 2) sera, respectively. Thereafter, immunoprecipitates were resolved by SDS-PAGE and immunoblots were screened with anti-HA 3F10 antibody to detect coimmunoprecipitation of HA-tagged p85^{DN}. B and D, HEK:HATPα cells (B, lanes 2, 3, and 5) and HEK:HATPβ cells (D, lanes 2, 3, and 5) or HEK 293 cells (B and D, lanes 1 and 4) were immunoprecipitated with anti-TPα (B, lanes 1 and 2), anti-TPβ (B, lane 3; D, lanes 1 and 3), or anti-HA 101R (B and D, lanes 4 and 5) antisera. Immunoprecipitates were resolved by SDS-PAGE and immunoblots were screened with anti-HA 3F10 antibody. E, immunoblot analysis of total cellular lysate (100 μg) by using anti-HA 3F10 antibody to confirm expression of HA-tagged p85^{DN} (lane 2) with nontransfected cells serving as a reference (lane 1). DN, dominant negative.

Effect of GF 109203X and H-89 on TPα- and TPβ-Mediated ERK Activation. Preincubation of HEK.TPα10 cells with the PKC inhibitor GF 109203X, at a previously established PKC-selective inhibitory concentration (Martiny-Baron et al., 1993), led to near complete inhibition of U46619-induced ERK1/2 activation (Fig. 4A). In HEK.TPβ3 cells, GF 109203X only partial inhibited U46619-mediated ERK1/2 activation (Fig. 4B). Specifically, GF 109203X pretreatment reduced U46619-mediated ERK activation in HEK.TPα10 cells from a 7.57 ± 0.45- to 2.15 ± 0.42-fold increase over basal levels (Fig. 4C; $n = 8$). However, in HEK.TPβ3 cells, U46619-mediated ERK activation was reduced from a 5.25 ± 0.36- to 3.11 ± 0.22-fold increase over basal levels (Fig. 4C; $n = 8$). Moreover, the effects of GF 109203X on U46619-induced ERK activation in HEK.TPα10 and HEK.TPβ3 cells were concentration-dependent (data not shown). Specifically, IC_{50} values of 206 and 840 nM GF 109203X were determined in HEK.TPα10 and HEK.TPβ3 cells, respectively. As a control, GF 109203X inhibited PMA-induced ERK activation, indicating that it was used at an effective, inhibitory concentration (Fig. 4, A and B).

Preincubation of quiescent HEK.TPα10 and HEK.TPβ3 cells with the potent PKA inhibitor H-89 (K_i = 48 nM), at a previously established inhibitory concentration (Daaka et al., 1997), significantly reduced U46619-mediated ERK1/2 activation but, as a control, had no effect on EGF-mediated ERK activation (Fig. 5, A–C). At higher concentrations, H-89 may inhibit other serine/threonine kinases, for example, PKC (K_i = 31.7 μM). However, we routinely use H-89 at a concentration below the K_i for PKC and have previously demonstrated that at the concentration used, PKA is inhibited, without effect on PKC (Walsh et al., 2000; Walsh and Kinsella, 2000). Additionally, the potent PKA inhibitor KT 5720 (1 μM; 45 min) significantly inhibited U46619-mediated ERK activation in HEK.TPα10 and HEK.TPβ3 cells (data not shown). In all cases, equal protein loading and equal ERK1 and ERK2 expression were confirmed for each sample by using an anti-ERK antibody (Figs. 4, A and B; 5, A and B, bottom). It has recently been reported that H-89 may as an antagonist of certain GPCRs, thereby calling into question its utility as a selective PKA inhibitor (Penn et al., 1999). To rule out the possibility that H-89 may act as an antagonist of the hTPs, we investigated the effect of H-89 on ligand binding by both the TPα and TPβ isoforms by using [^{3}H]SQ29,548 as selective TP radioligand. In keeping with our previous reports (Walsh et al., 2000), H-89 had no affect on ligand binding by either TPα or TPβ isoforms. Specifically, HEK.TPα10 cells exhibited 1.97 ± 0.42 and 2.25 ± 0.42 pmol of [^{3}H]SQ29,548 bound/mg of protein in the absence and presence of 10 μM H-89, respectively. HEK.TPβ3 cells exhibited 1.93 ± 0.13 and 2.09 ± 0.01 pmol of [^{3}H]SQ29,548 bound/mg of protein in the absence and presence of H-89, respectively.

Role of A-Raf, c-Raf, and Rap1b in TPα- and TPβ-Mediated ERK Activation. Coexpression of the DN forms of either A-Raf (A-Raf^{DN}) or c-Raf (c-Raf^{DN}) decreased U46619-mediated ERK activation in both HEK.TPα10 and HEK.TPβ3 cells but did not affect the level of basal ERK activation in either cell type (Fig. 6, A and B). Overexpression of both A-Raf^{DN} and c-Raf^{DN} were confirmed by western blot analyses (Fig. 6D). Additionally, HEK.TPα10 and HEK.TPβ3 cells transiently transfected with either A-Raf^{DN} or c-Raf^{DN} neither elicited ERK activation in the absence of U46619

(Fig. 6, A and B) nor demonstrated altered levels of TP expression compared with control nontransfected cells (data not shown).

To establish whether the Rap1b/B-Raf signaling system (Schmitt and Stork, 2000) may play a role in TP-mediated ERK activation, the effect of its DN form $Rap1b^{S17N}$ ($Rap1b^{N17}$; Schmitt and Stork, 2000) on U46619-mediated ERK activation was investigated. Coexpression of $Rap1b^{N17}$ resulted in a partial inhibition of U46619-mediated ERK activation in both HEK.TPα10 and HEK.TPβ3 cells (Fig. 7, A–C). For each independent experiment, overexpression of $Rap1b^{N17}$ was confirmed by Western blot analysis (data not shown). Additionally, HEK.TPα10 and HEK.TPβ3 cells transiently transfected with $Rap1b^{N17}$ neither elicited ERK activation in the absence of U46619 (Fig. 7, A and B) nor exhibited altered levels of TP expression compared with control nontransfected cells (data not shown).

Role of Class I_B PI3K in TPα- and TPβ-Mediated ERK Activation. Pretreatment of quiescent HEK.TPα10 and HEK.TPβ3 cells with the PI3K inhibitor wortmannin, at an established PI3K-selective inhibitory concentration (Leopoldt et al., 1998), led to near complete inhibition of U46619-mediated ERK activation (Fig. 8, A and C). Moreover, pretreatment of HEK.TPα10 and HEK.TPβ3 cells with the more selective PI3K inhibitor LY294002, at an established inhibitory concentration (Vlahos et al., 1994), also significantly inhibited U46619-mediated ERK activation compared with cells exposed exclusively to U46619 under similar conditions (Fig. 8, A–C).

Coexpression of $PI3K\gamma^{DN}$ (with/without the adaptor subunit p101; data not shown) did not affect U46619-induced activation of ERK in either HEK.TPα10 or HEK.TPβ3 cells compared with vehicle-treated cells (Fig. 9, A–D). Moreover, transient overexpression of either the β-ARK1 (495–689) minigene, to sequester G$\beta\gamma$ subunits (Koch et al., 1994), or the Gβ1γ2 subunit did not affect U46619-mediated ERK activation in HEK.TPα10 or HEK.TPβ3 cells (Fig. 9, A–D). Pretreatment of quiescent HEK.TPα10 and HEK.TPβ3 cells with pertussis toxin (PTx), at a concentration established to inhibit $G\alpha_i$ signaling (Lawler et al., 2001; data not shown), did not affect U46619-induced ERK1/2 activation compared with cells treated with U46619 alone (Fig. 9, A–D). Additionally, HEK.TPα10 and HEK.TPβ3 cells transiently transfected with either the $PI3K\gamma^{DN}$ or the β-ARK1(495-689) minigene or the Gβ1γ2 subunit did not elicit ERK activation in the absence (−) of U46619 (Fig. 9, A–D). In all cases, equal protein loading and equal ERK1/2 expression was confirmed using an anti-ERK antibody (Fig. 9, A and B, bottom). For each independent experiment, transient overexpression of G$\beta\gamma$, β-ARK and $PI3K\gamma^{DN}$ was confirmed by Western blot analyses (data not shown).

Role of Class I_A PI3K in TPα- and TPβ-Mediated ERK Activation. Because the G$\beta\gamma$-regulated class 1_B subfamily of

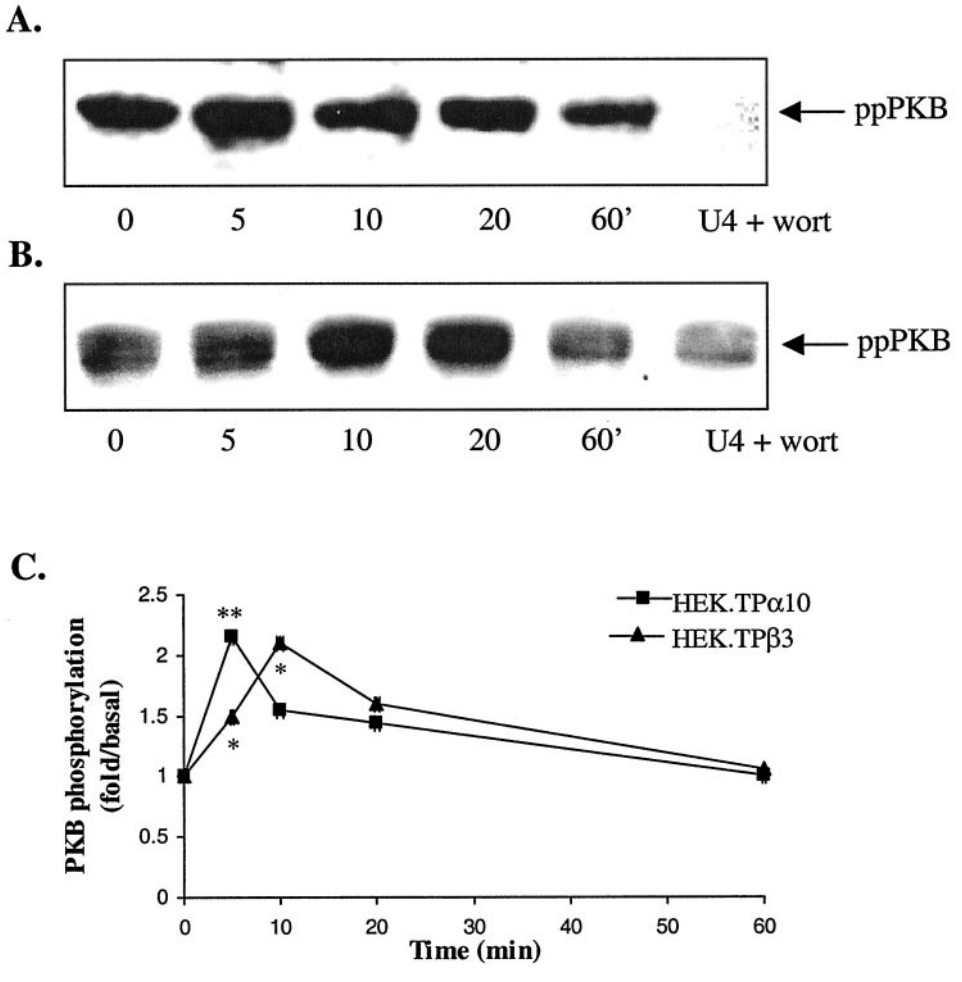

Fig. 12. Time-dependent effect of U46619 on PKB activation in HEK.TPα10 and HEK.TPβ3 cells. HEK.TPα10 (A) and HEK.TPβ3 (B) cells were stimulated for 0 to 60 min with 100 nM U46619. Additionally, in A (HEK.TPα10 cells) and B (HEK.TPβ3 cells), cells were preincubated with wortmannin (wort; 400 nM; 30 min) before stimulation of cells with U46619 (100 nM; 5 min). A and B, blots were screened with anti-phosphorylation-specific PKB to detect the phosphorylated, active forms of PKB (ppPKB). Results are representative of three independent experiments. C, fold increases in PKB (ppPKB) phosphorylation in A (HEK.TPα10 cells) and B (HEK.TPβ3 cells), respectively, are presented as mean fold increases of basal PKB phosphorylation ± S.E.M. (n = 3), where the levels of basal PKB phosphorylation in vehicle-treated cells are assigned a value of 1.0. *, $p \leq 0.05$ and **, $p \leq 0.01$) indicate that the levels of U46619-mediated PKB activation (ppPKB) were significantly greater compared with basal levels.

PI3K does not seem to be involved in TP-mediated ERK activation, the role of PI3K class 1_A was investigated. Coexpression of a dominant negative form of the class 1_A adaptor subunit ($p85^{DN}$; Sutor et al., 1999) resulted in a marginal decrease in U46619-mediated ERK activation in both HEK.TPα10 and HEK.TPβ3 cells (Fig. 10, A–C). In addition, overexpression of the wild-type p85 in both HEK.TPα10 and HEK.TPβ3 cells augmented U46619-mediated ERK activation (data not shown).

Thereafter, to investigate whether the p85 subunit may directly associate with the TP isoforms, coimmunoprecipitation of TPα and TPβ with p85 was investigated using TP isoform-specific antisera directed to residues within the unique C-tails of TPα and TPβ (Miggin and Kinsella, 2001). Association of the wild-type p85 (data not shown) and $p85^{DN}$ with both TPα and TPβ was confirmed by the coimmunoprecipitation of the HA-tagged p85 with the anti-TP antisera (Fig. 11, A and C, lane 1). However, coimmunoprecipitation of p85 with either TPα or TPβ did not occur with the respective TP preimmune sera (Fig. 11, A and C, lane 2). Moreover, as an additional confirmation of coimmunoprecipitation of p85 with either TPα or TPβ, initial immunoprecipitation of HA-tagged p85 from HEK.TPα10 and HEK.TPβ3 cells with the anti-HA 101r antisera resulted in coimmunoprecipitation of both TPα or TPβ, as detected using their respective isoform specific antisera (data not shown).

To demonstrate the specificity of the TPα and TPβ antisera, HA-tagged TPs were immunoprecipitated with anti-TPα antisera, anti-TPβ antisera, and, as a control, with the anti-HA 101r antibody directed to the HA-epitope tag. Immunoprecipitations of HA-tagged TPα and TPβ were confirmed by back blotting with the anti-HA 3F10-POD-conjugated antibody (Fig. 11, B and D, lane 5). Although the anti-TPα antisera resulted in the immunoprecipitation of a broad protein band corresponding to the glycosylated and nonglycosylated forms of TPα, anti-TPβ antisera did not immunoprecipitate TPα (Fig. 11B; compare lane 2 to 3, respectively). Similarly, although the anti-TPβ antisera resulted in the immunoprecipitation of a broad protein band corresponding to the glycosylated and nonglycosylated forms of TPβ, the anti-TPα antisera did not immunoprecipitate TPβ (Fig. 11D; compare lane 3 to 2, respectively). Taken together, these data confirm the specificity of the anti-TP antisera and suggest that PI3K class 1_A can interact with both TPα and TPβ to mediate ERK activation.

As an extension of these studies, to establish whether TPα and TPβ may, in turn, stimulate PKB/Akt activation in response to PI3K activation, the effect of U46619 on PKB activation was examined. Exposure of HEK.TPα10 and HEK.TPβ3 cells to U46619-induced time-dependent activations of PKB with maximal phosphorylation observed at 5 min (Fig. 12, A and C) and at 10 to 20 min (Fig. 12, B and C), respectively. In addition, U46619-induced activation of PKB in HEK.TPα10 and HEK.TPβ3 cells was attenuated when cells were preincubated with the PI3K inhibitors wortmannin (Fig. 12, A and B) and LY294002 (data not shown).

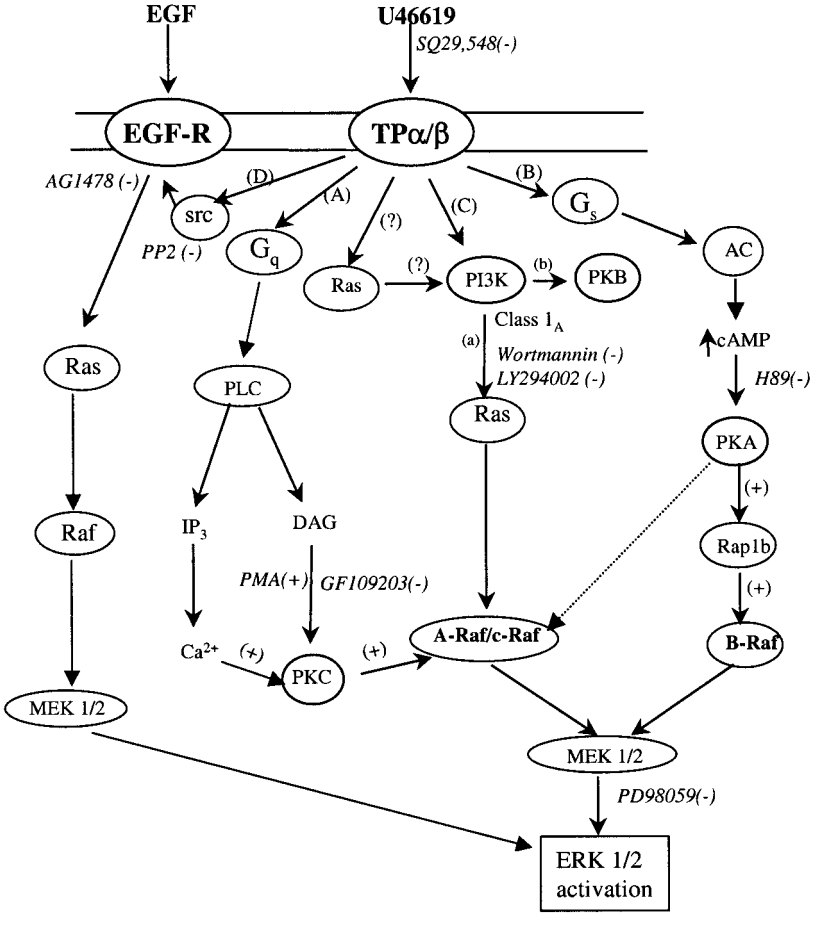

Fig. 13. Proposed model for TP-mediated mitogen-activated protein kinase activation. A, ligand activation of the TXA_2 receptor TPα and TPβ isoforms leads to Gq-mediated activation of PLC, leading to increases in intracellular concentrations of IP_3 and DAG, and concomitant activation of Ca^{2+}-sensitive, DAG-regulated PKC. A key target of PKC is its positive regulation of c-Raf and, to a lesser extent, A-Raf leading to mitogen-activated protein kinase kinase 1 and 2 phosphorylation and activation of ERK1 and -2. B, in addition, ligand activation of TPα and TPβ may lead to Gs-dependent activation of adenylyl cyclase (AC) resulting in increases in intracellular concentrations of cAMP and, in turn, activation of H-89-sensitive PKA. PKA may, in turn, phosphorylate c-Raf to inhibit its actions but may also phosphorylate Rap1b, which, in turn, sequesters B-Raf leading to sustained activation of B-Raf, leading to ERK activation. C, ligand activation of TPα and TPβ may also signal through activation of wortmannin and LY294002-sensitive PI3K class 1_A members, through unknown mechanisms but which may involve direct interaction of TPα and TPβ with the p85 adaptor subunit, leading to Ras signaling and ERK activation (a) and leading to PKB activation (b). D, ligand activation of TPα and TPβ may also signal through transactivation of AG1478-sensitive epidermal growth factor receptor (EGF-R) through an unknown mechanisms involving PP2-sensitive src, leading to activation of ERK1 and -2. Although the TP antagonist SQ29,548 completely inhibits TP-mediated mitogenesis, PTx, G$\beta\gamma$ subunits, and βARK1(495-689) minigene are without an effect on this pathway. Solid arrows and/or (+) indicate positive effects; broken lines and/or (−) indicate inhibitory effects. ? indicates whether PI3K acts as upstream or downstream of ras.

Discussion

TXA_2 has been implicated as a positive mediator of mitogenic/hypertrophic responses in vascular smooth muscle (Morinelli et al., 1994). Both the TXA_2 mimetics [1*S*-[1α,2α(*Z*), 3β(1*E*,3*S**),4α]]-7-[3-[3-hydroxy-4-(4-iodophenoxy)-1-butenyl]-7-oxabicyclo[2.2.1]hept-2-yl]-5-heptenoic acid and U46619 activate ERK1/2 in porcine, rat, and bovine aortic SMCs, respectively (Morinelli et al., 1994; Jones et al., 1995; Grosser et al., 1997), although the mechanisms of ERK activation remain poorly defined. Recently, Gao et al. (2001) reported that TP-mediated ERK activation in human endothelial ECV304 cells involved transactivation of the EGF receptor. They proposed that TP-mediated mitogenesis occurred in a PTx-sensitive, $G_{i/o}$-src-EGF receptor-dependent mechanism (Gao et al., 2001). In another study in cultured human uterine SMCs, we have established that TP-mediated ERK activation in response to U46619 and the F2 isoprostane 8-epi $PGF_{2\alpha}$ also involves transactivation of the EGF receptor; however, ERK activation was insensitive to PTx but occurred in a PKA-, PKC-dependent manner in a pathway that also required the participation of PI3K (Miggin and Kinsella, 2001). Thus, it seems that there are differences in TP-mediated ERK activation in human endothelial and in human uterine SMCs, readily distinguishable on the basis of their apparent sensitivity to PTx and the requirement for other signaling elements in human SMCs. Thus, in the current study, we first sought to fully define the mechanisms leading to TXA_2-mediated ERK activation. Second, we sought to establish whether the individual TPα and TPβ receptor isoforms regulate ERK signaling and to define the key elements of those cascade(s).

In the present study, the previously described HEK 293 cell lines stably overexpressing either TPα (HEK.TPα10) or TPβ (HEK.TPβ3) (Walsh et al., 1998, 2000) were used to investigate the mechanisms of TPα- and TPβ-mediated ERK signaling. U46619 elicited concentration- and time-dependent activations of ERK1/2 through both TPα and TPβ. Maximal U46619-induced ERK activations in HEK.TPα10 and in HEK.TPβ3 cells were observed at 10 and 5 min, respectively. The relevance of differential rates of ERK activation through the TP isoforms remains to be determined, but may be related to a requirement for rapid ERK activation through TPβ in certain tissues that express higher levels of this isoform, for example, fetal vascular smooth muscle (Miggin and Kinsella, 1998).

The role of Ras in GPCR-mediated activation of the ERK signaling cascade is well documented. Indeed, U46619 induced rapid Ras activation platelets (Shock et al., 1997). In this study, overexpression of Ha-Ras augmented U46619-induced ERK activation in both HEK.TPα10 and HEK.TPβ3 cells, whereas overexpression of dominant negative Ha-Ras^{N17} partially inhibited U46619-induced ERK activation in both cell lines. Concurring with findings in uterine SMCs and ECV304 cells (Gao et al., 2001; Miggin and Kinsella, 2001), we have also established that both TPα- and TPβ-mediated ERK activation involves transactivation of the EGF receptor, and is src-dependent.

Previous studies have demonstrated that PKC activation was necessary for TXA_2-stimulated hypertrophic growth in vascular smooth muscle (Craven et al., 1996) and that U46619-induced activation of Ras in platelets was PKC-dependent (Shock et al., 1997). Furthermore, inhibition of GF 109203X-sensitive PKCs led to a decrease in U46619-induced ERK activation in cultured human SMCs (Miggin and Kinsella, 2001). Thus, the role of PKC in U46619-mediated activation of ERK through both TPα and TPβ was investigated. In contrast to the strong PKC-dependent activation of ERK in HEK.TPα10 cells, U46619-induced ERK activation in HEK.TPβ3 cells was only partially dependent on GF 109203X-sensitive PKCs. The precise mechanism of the differential PKC dependence of TXA_2-induced ERK activation through either TPα or TPβ remains to be fully investigated; however, it is possible that the TP isoforms may represent differential targets of PKC isoform activation. In keeping with this, we have previously established that the TPα and TPβ isoforms are subject to differential PGE_2-induced desensitization in a mechanism most probably involving direct PKC phosphorylation of the TP isoforms within their unique C-tail domains (Walsh and Kinsella, 2000).

Typically, increased levels of intracellular cAMP were thought to attenuate the ERK signaling cascade (Burgering et al., 1993). Recent evidence now suggests that, in certain situations, elevations of cAMP may actually activate the ERK signaling cascade (Frödin et al., 1994), through both the $G\alpha_S$ subunit and the $G_{\beta\gamma}$ subunits of the activated G_S (Faure et al., 1994). Interestingly, correlating with findings in human uterine SMCs and in COS-7 cells (Faure et al., 1994; Miggin and Kinsella, 2001), we found that U46619-induced ERK activation was partially dependent on PKA, because H-89 significantly decreased ERK activation through both TPα and TPβ.

Taken together, our studies have shown that both PKC and PKA are involved in ERK activation through the TP isoforms. It is postulated that the positive effects of PKC may be mediated through any one of the PKC-sensitive Raf isozymes, such as c-Raf (Anton and Wennogle, 1998). However, because c-Raf is inhibited by PKA, it is also postulated that other Raf isoforms may be involved in TXA_2-mediated ERK activation. To address this question, the direct role of A-Raf and c-Raf in TP-mediated ERK activation was examined. Both the PKA-insensitive A-Raf and the PKA-sensitive c-Raf were demonstrated to regulate U46619-induced ERK activation through TPα and TPβ. Additionally, overexpression of $Rap1b^{N17}$ significantly reduced ERK activation through TPα and TPβ, suggesting that the somewhat novel PKA-modulated Rap1/B-Raf mechanism of ERK regulation (Schmitt and Stork, 2000) may also be involved in TP-mediated ERK activation. The availability of dominant negative forms of B-Raf would add further clarification to this point.

GPCRs have been shown to regulate the class I family of PI3Ks (Vanhaesebroeck et al., 1997), although a mechanism has not yet been clearly defined. In the current study, using the PI3K inhibitors wortmannin and LY294002, we have shown that ERK activation via TPα and TPβ is mediated through PI3K, correlating with findings in human uterine SMCs (Miggin and Kinsella, 2001). Additionally, the dominant negative $PI3K\gamma^{K832P}$ (Lopez-Ilasaca et al., 1998) did not affect U46619-mediated ERK activation in either cell type. Moreover, overexpression of Gβ1γ2 or the G$\beta\gamma$ antagonist β-ARK1(495-689) minigene (Koch et al., 1994) did not affect ERK activation through TPα and TPβ. Additionally, PTx did not affect ERK activation through TPα and TPβ. These data

suggest that PI3K class 1_B is not involved in TP-mediated ERK activation.

In previous studies, Morinelli et al. (1997) demonstrated that exposure of A7r5 cells overexpressing TPα to I-BOP led to tyrosine phosphorylation of both the TPα itself and the p85 adaptor subunit of class I_A PI3Ks. In view of these findings and our studies indicating a specific role for wortmannin- and LY294002-sensitive PI3Ks, distinct from the class 1_B family, we sought to investigate a possible role of class I_A PI3Ks in TPα- and TPβ-mediated ERK activation. Overexpression of a dominant negative form of PI3K class 1_A adaptor subunit, $p85^{DN}$ (Sutor et al., 1999), partially inhibited U46619-induced ERK activation, indicating that p85 is involved in TP-mediated ERK activation. The finding that $p85^{DN}$ only partially inhibited TP-mediated ERK activation can most probably be explained by the high endogenous levels of p85 in HEK 293 cells (Dr. Len Stephens, Babraham Institute, Cambridge, UK; personal communication). Moreover, TP isoform-specific antisera, but not the preimmune sera, permitted immunoprecipitation of both the wild-type p85 (data not shown) and the $p85^{DN}$, confirming association of both TPα and TPβ with PI3K class 1_A $p85^{DN}$ adaptor subunit. Additionally, initial immunoprecipitation of HA-tagged p85 resulted in coimmunoprecipitation of both TPα and TP (data not shown). Although the precise mechanism of TP:p85 association remains to be defined, the fact that the $p85^{DN}$, devoid of a portion of the intracellular SH2 domain (Sutor et al., 1999), could associate with both TPα and TPβ indicates that other domains, such as the amino (N) or carboxyl (C) terminal SH2 domains of p85, are involved (Wymann and Pirola, 1998). Our studies do not, however, exclude the possibility that other (adaptor) protein(s) may mediate association of TPα/TPβ with p85.

Thus, through these studies, we provide novel evidence suggesting that class 1_A, not class 1_B, PI3K mediates ERK activation through TPα and TPβ. Several studies have indicated that PKB/Akt activation is a key event in the realization of the antiapoptotic effect of PI3K (Datta et al., 1999). Through follow-up studies, we established that TPα and TPβ induced activation of PKB/Akt through wortmannin- and LY294002-sensitive phosphorylation of PKB (S^{473}). Thus, in keeping with its mitogenic actions, it seems that TXA_2 and its mimetics may not only promote mitogenesis through activation of the ERK cascade but also may stimulate antiapoptotic signaling through activation of PKB and its downstream signaling. These findings contrast those of Gao et al. (2000) who demonstrated that I-BOP partially inhibited PKB activation in cultured ECV304 cells. An explanation of these conflicting data will require further investigation but may possibly be attributed to differences in the cell type under study.

In summary, based on the current general understanding of ERK signal transduction cascades, we now propose a model of TXA_2-mediated ERK activation (Fig. 13). The TP agonist U46619 induces ERK activation through both TPα and TPβ in a concentration- and time-dependent manner. TP-dependent ERK activation involves transactivation of the EGF receptor, in a mechanism possibly involving src, but is also dependent on PKA-, PKC-, and PI3K-mediated signaling. In view of the strong dependence of PKA on TP-mediated ERK activation coupled to the fact that EGF signaling may be inhibited by PKA through direct phosphorylation of the EGF receptor itself (Barbier et al., 1999), it is unlikely that all of the downstream effects of U46619-mediated ERK activation are EGF-dependent.

Although TPα-mediated ERK activation is dependent on DAG-activated PKCs, TPβ-mediated ERK activation is only partially dependent on DAG-activated PKCs. Ras, PI3K class 1_A, but not class 1_B, and the Raf isoforms c-Raf, A-Raf, and PKA-regulated Rap1/B-Raf transduce U46619-mediated ERK activation through both TPα and TPβ. Additionally, PKB/Akt was shown to be activated in a PI3K-dependent manner. In our proposed model (Fig. 13), our data are in partial agreement with those of Gao et al. (2001) in that TP-mediated ERK activation involves transactivation of the EGF receptor; however, our study expands this mechanism and indicates the clear involvement of additional PKA-, PKC-, and PI3K-dependent, PTx-independent mechanisms not identified by those studies in ECV304 cells (Gao et al., 2001). Thus, it is clear that the regulation of the ERK signaling cascades through TPα and TPβ is multifaceted with multiple intermediates participating in this highly regulated signaling network, and studies presented herein have identified the key components involved in the regulation of TXA_2-mediated ERK activation.

References

Anton Y and Wennogle LP (1998) The RAF family: an expanding network of post-translational controls and protein-protein interactions. *Cell Res* **8:**81–98.

Barbier AJ, Poppleton HM, Yigzaw Y, Mullenix JB, Wiepz GJ, Bertics PJ, and Patel TB (1999) Transmodulation of epidermal growth factor receptor function by cyclic AMP-dependent protein kinase. *J Biol Chem* **274:**14067–14073.

Bogoyevitch M, Glennon P, Andersson M, Clerk A, Lazou A, Marshall C, Parker P, and Sugden P (1994) Endothelin-1 and fibroblast growth factors stimulate the mitogen-activate protein kinase signalling cascade in cardiac myocytes. *J Biol Chem* **269:**1110–1119.

Boulton TG, Gregory JS, and Cobb MH (1991) Purification and properties of extracellular signal-regulated kinase 1, an insulin-stimulated microtubule-associated protein 2 kinase. *Science (Wash DC)* **249:**64–67.

Burgering B, Pronk G, Van Weeren C, Chardin P, and Bos J (1993) cAMP antagonises $p21^{ras}$-directed activation of extracellular signal-regulated kinase 2 and phosphorylation of mSos nucleotide exchange factor. *EMBO (Eur Mol Biol Organ) J* **12:**4211–4220.

Coso OA, Chiariello M, Yu JC, Termoto H, Crespo P, Xu N, Miki T, and Gutkind JS (1995) The small GTP-binding proteins rac-1 and cdc-42 regulate the activity of the JNK/SAPK signalling pathway. *Cell* **81:**1137–1146.

Craven PA, Studer RK, and DeRubertis FR (1996) Thromboxane/prostaglandin endoperoxide-induced hypertrophy of rat vascular smooth muscle cells is signalled by protein kinase C-dependent increases in transforming growth factor-β. *Hypertension* **28:**169–176.

Daaka Y, Luttrell L, and Lefkowitz R (1997) Switching of the coupling of the β_2-adrenergic receptor to different G proteins by protein kinase A. *Nature (Lond)* **390:**88–91.

Datta SR, Brunet A, and Greenberg ME (1999) Cellular survival: a play in three Akts. *Genes Dev* **13:**2905–2927.

Faure M, Voyno-Ysenetskayac T, and Bourne H (1994) cAMP and $\beta\gamma$ subunits of heterotrimeric G-proteins stimulate the mitogen-activated protein kinase pathway in COS-7 cells. *J Biol Chem* **269:**7851–7854

Frödin M, Peraldi P, and Van Obberghen E (1994) Cyclic AMP activates the mitogen-activated protein kinase cascade in PC12 cells. *J Biol Chem* **269:**6207–6214.

Gao Y, Tang S, Zhou S, and Ware JA (2001) The thromboxane A2 receptor activates mitogen-activated protein kinase via protein kinase C-dependent Gi coupling and Src-dependent phosphorylation of the epidermal growth factor receptor. *J Pharmacol Exp Ther* **296:**426–433.

Gao Y, Yokota R, Tang S, Ashton AW, and Ware JA (2000) Reversal of angiogenesis in vitro, induction of apoptosis and inhibition of Akt phosphorylation in endothelial cells by thromboxane A_2. *Circ Res* **87:**739–745.

Grosser T, Zucker T, Weber A, Schulte K, Sachinidis A, Vetter H, and Schror K (1997) Thromboxane A_2 induces cell signalling but requires platelet-derived growth factor to act as a mitogen. *Eur J Pharmacol* **319:**327–332.

Hagemann C and Rapp UR (1999) Isotype-specific functions of raf kinases. *Exp Cell Res* **253:**34–46.

Jones D, Benjamin C, and Linseman D (1995) Activation of thromboxane and prostacyclin receptors elicits opposing effects on vascular smooth muscle cell growth and mitogen-activated protein kinase signalling cascades. *J Pharmacol Exp Ther* **48:**890–896.

Kinsella BT (2001) Thromboxane A_2 signalling in humans: a 'tail' of two receptors. *Biochem Soc Trans* **29:**641–654.

Kinsella BT, Erdman R, and Maltese W (1991) Posttranslational modification of Ha-ras by farnesyl versus geranylgeranyl isoprenoids is determined by the COOH-terminal amino acid. *Proc Natl Acad Sci USA* **88:**8934–8938.

Koch WJ, Hawes BE, Inglese J, Luttrell LM, and Lefkowitz RJ (1994) Cellular expression of the carboxyl terminus of a protein-coupled receptor kinase attenuates $G_{\beta\gamma}$-mediated signalling. *J Biol Chem* **269:**6193–6197.

Lawler OA, Miggin SM, and Kinsella BT (2001) Protein kinase A dependent phosphorylation of serine 357 of the mouse prostacyclin receptor regulated its coupling to Gs-, Gi- and to Gq-coupled effector signalling. *J Biol Chem* **276:**33596–33607.

Leopoldt D, Hanck T, Exner T, Maier U, Wetzker R, and Nurnberg B (1998) G$\beta\gamma$ stimulates phosphoinositide 3-kinase-γ by direct interaction with two domains of the catalytic p110 subunit. *J Biol Chem* **273:**7024–7029.

Lopez-Ilasaca M, Gutkind JS, and Wetzker R (1998) Phosphoinositide 3-kinase γ is a mediator of G$\beta\gamma$-dependent jun kinase activation. *J Biol Chem* **273:**2505–2508.

Martiny-Baron G, Kazanietz MG, Mischak H, Blumberg PM, Kochs G, Hug H, Marme D, and Schachtele C (1993) Selective inhibition of protein kinase C isozymes by the indolocarbazole Go 6976. *J Biol Chem* **268:**9194–9197.

Miggin SM and Kinsella BT (1998) Expression and tissue distribution of the mRNAs encoding the human thromboxane A_2 receptor (TP) alpha and beta isoforms. *Biochim Biophys Acta* **1425:**543–559.

Miggin SM and Kinsella BT (2001) Thromboxane A_2 receptor mediated activation of the mitogen activated protein kinase cascades in human uterine smooth muscle cells. *Biochim Biophys Acta* **1539:**147–162.

Morinelli TA, Finley EL, Jaffa AA, Kurtz DT, and Ullian ME (1997) Tyrosine phosphorylation of phosphatidylinositol 3-kinase and of the thromboxane A_2 (TXA_2) receptor by the TXA_2 mimetic I-BOP in A7r5 cells. *Biochem Pharmacol* **53:**1823–1832.

Morinelli TA, Zhang LM, Newman WH, and Meier KE (1994) Thromboxane A_2/prostaglandin H_2-stimulated mitogenesis of coronary artery smooth muscle cells involves activation of mitogen-activated protein kinase and S6 kinase. *J Biol Chem* **269:**5693–5698.

Narumiya S, Sugimoto Y, and Fumitaka U (1999) Prostanoid receptors: structures, properties, and functions. *Physiol Rev* **79:**1193–1226.

Penn RB, Parent JL, Pronin AN, Panettieri RA, Jr, and Benovic JL (1999) Pharmacological inhibition of protein kinases in intact cells: antagonism of beta adrenergic receptor ligand binding by H-89 reveals limitations of usefulness. *J Pharmacol Exp Ther* **288:**428–437.

Schmitt JM and Stork PJS (2000) β_2-adrenergic receptor activates extracellular signal regulated kinases (ERKs) via the small G-protein rap1 and the serine/threonine kinase B-raf. *J Biol Chem* **275:**25342–25350.

Shock DD, He K, Wencel-Drake JD, and Parise LV (1997) Ras activation in platelets after stimulation of the thrombin receptor, thromboxane A_2 receptor or PKC. *Biochem J* **321:**525–530.

Sugden PH and Clerk A (1997) Regulation of the ERK subgroup of MAP kinase cascades through G protein-coupled receptors. *Cell Signal* **9:**337–351.

Sutor S, Vroman B, Armstrong E, Abraham R, and Karnitz L (1999) A phosphatidylinositol 3-kinase-dependent pathway that differentially regulates c-raf and a-raf. *J Biol Chem* **274:**7002–7010.

Vanhaesebroeck B, Leevers S, Panayotou G, and Waterfield M (1997) Phosphoinositide 3-kinases: a conserved family of signal transducers. *Trends Biochem Sci* **22:**267–272.

Vlahos CJ, Matter WF, Hui KY, and Brown RF (1994) A specific inhibitor of phosphatidylinositol 3-kinase, 2-(4-morpholinyl)-8-phenyl-4*H*-1-benzopyran-4-one (LY294002). *J Biol Chem* **269:**5241–5248.

Walsh MT, Foley JF, and Kinsella BT (1998) Characterization of the role of N-linked glycosylation on the cell signaling and expression of the human thromboxane A_2 receptor alpha and beta isoforms. *J Pharmacol Exp Ther* **286:**1026–1036.

Walsh MT, Foley JF, and Kinsella BT (2000) The α, but not the β, isoform of the human thromboxane A_2 receptor (TP) is a target for prostacyclin mediated desensitization. *J Biol Chem* **275:**20412–20423.

Walsh MT and Kinsella BT (2000) Regulation of the human prostanoid TPα and TPβ receptor isoforms mediated through activation of the EP_1 and IP receptors. *Br J Pharmacol* **131:**601–609.

Wang J, Auger K, Jarvis L, Shi Y, and Roberts T (1995) Direct association of Grb2 with the p85 subunit of phosphatidylinositol 3-kinase. *J Biol Chem* **270:**12774–12780.

Wymann MP and Pirola L (1998) Structure and function of phosphoinositide 3-kinases. *Biochim Biophys Acta* **1436:**127–150.

Address correspondence to: B. Therese Kinsella, Department of Biochemistry, Conway Institute of Biomolecular and Biomedical Research, Merville House, University College Dublin, Belfield, Dublin 4, Ireland. E-mail: therese.kinsella@ucd.ie